Study of the anomalous magnetic behavior of nanostructures by X-ray magnetic circular dichroism

Rogerio Magalhães-Paniago[#,*],

#Departamento de Física, UFMG, Belo Horizonte, Brazil
** Laboratório Nacional de Luz Síncrotron, Campinas SP, Brazil*

UFMG

LNLS

Overview

1. Tutorial: what is X-ray Magnetic Circular Dichroism
2. Scientific cases:
   - A. Anomalous Palladium magnetism in nanostructures
   - B. Giant orbital magnetic moment of Co/Au nanostructures
   - C. Magnetic domain reconfiguration in MnAs/GaAs films
   - D. Fe/MnAs magnetic coupling
   - E. Microscopy with magnetic domain sensitivity
4. Conclusion

1. Tutorial: what is X-ray Magnetic Circular Dichroism (XMCD)

XMCD reflects the dependence of photon absorption of a material on polarization. X-ray absorption spectroscopy utilizes the energy dependent absorption of x-rays to obtain information about the elemental composition

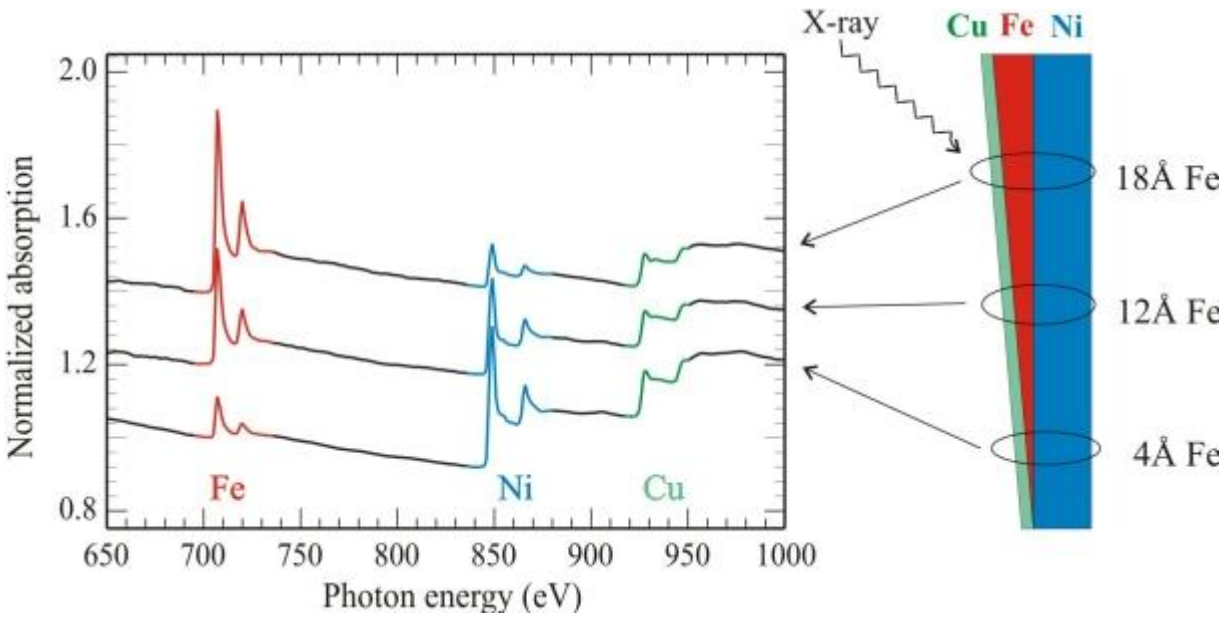

X-ray absorption spectra of a wedge sample, revealing the chemical composition

UFMG

LNLS

1. Tutorial: what is X-ray Magnetic Circular Dichroism (XMCD)

It also gives information on the chemical environment of the atoms and their magnetic state. Core electrons are excited in the absorption process into empty states above the Fermi energy and thereby probe the electronic and magnetic properties of the empty valence levels.

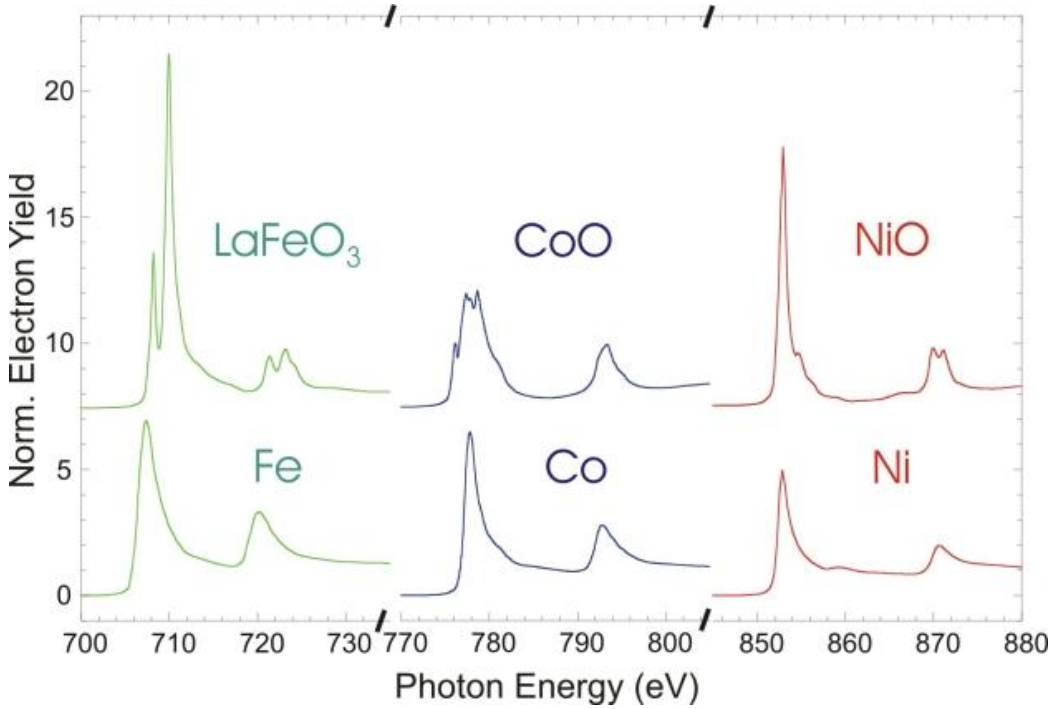

L-edge x-ray absorption edge spectra of Fe, Co and Ni in the form of the elemental metals and as oxides. They two main structures are called the L3 (lower energy) and L2 absorption edges. The two main peaks in the spectra arise from the spin orbit intera ction of the 2p core shell and the total intensity of the peaks is proportional to the number of empty 3d valence states.

UFMG

LNLS

1. Tutorial: what is X-ray Magnetic Circular Dichroism (XMCD)

The metals are usually ferromagnetic and their magnetic properties are best studied with X-Ray Magnetic Circular Dichroism spectroscopy, while the oxides are usually antiferromagnetic and are studied with X-Ray Magnetic Linear Dichroism.

Circular Dichroism - Ferromagnets

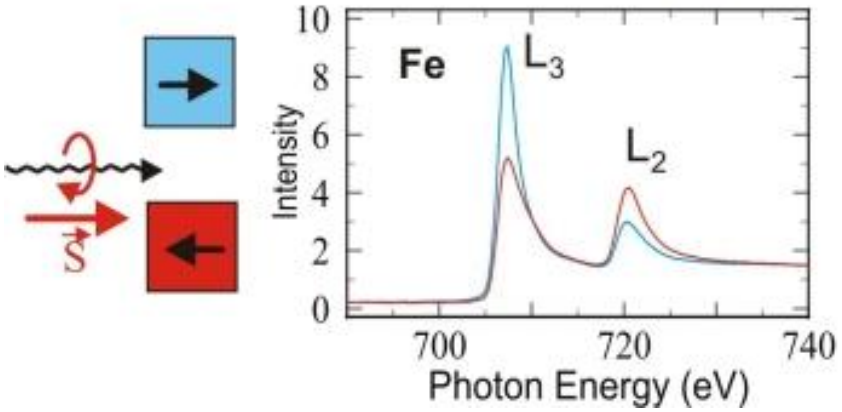

Linear Dichroism - Antiferromagnets

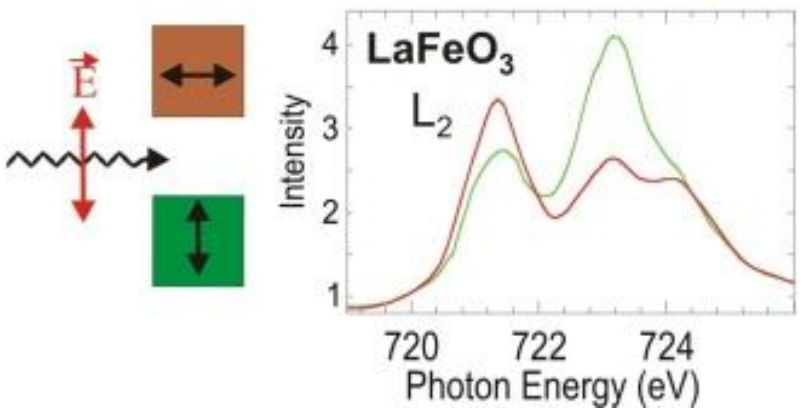

UFMG

LNLS

1. Tutorial: The concept of XMCD – Spin and Orbital Moments

- X-ray absorption process → spin dependent
- Use of right or left circularly polarized photons → transfer angular momentum to the excited photoelectron
- $p_{3/2}$ (L3) and $p_{1/2}$ (L2) levels have opposite spin-orbit coupling → spin polarization opposite at the two edges

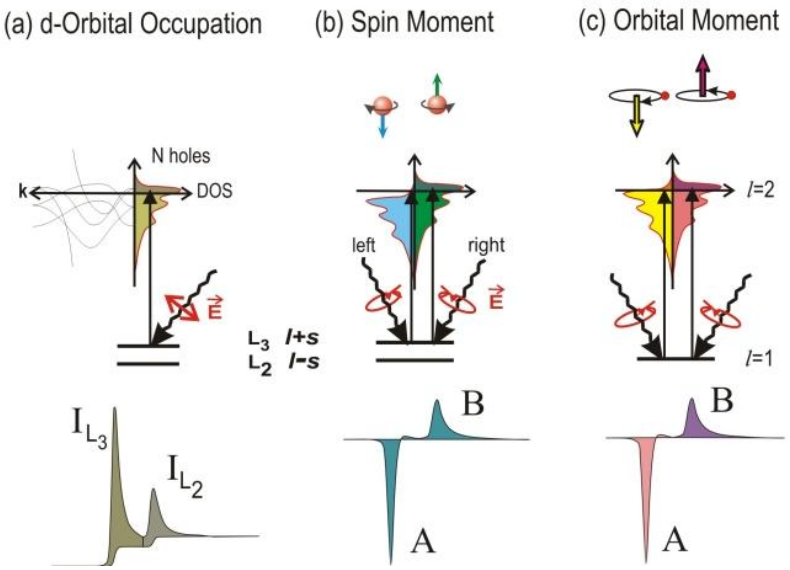

Electronic transitions in conventional L-edge x-ray absorption (a), and x-ray magnetic circular x-ray dichroism (b,c), illustrated in a one-electron model. The transitions occur from the spin-orbit split 2p core shell to empty conduction band states. By use of circularly polarized x-rays the spin moment (b) and orbital moment (c) can be determined from linear combinations of the dichroic difference intensities A and B, according to other sum rules.

1. Tutorial: The concept of XMCD – Spin and Orbital Moments

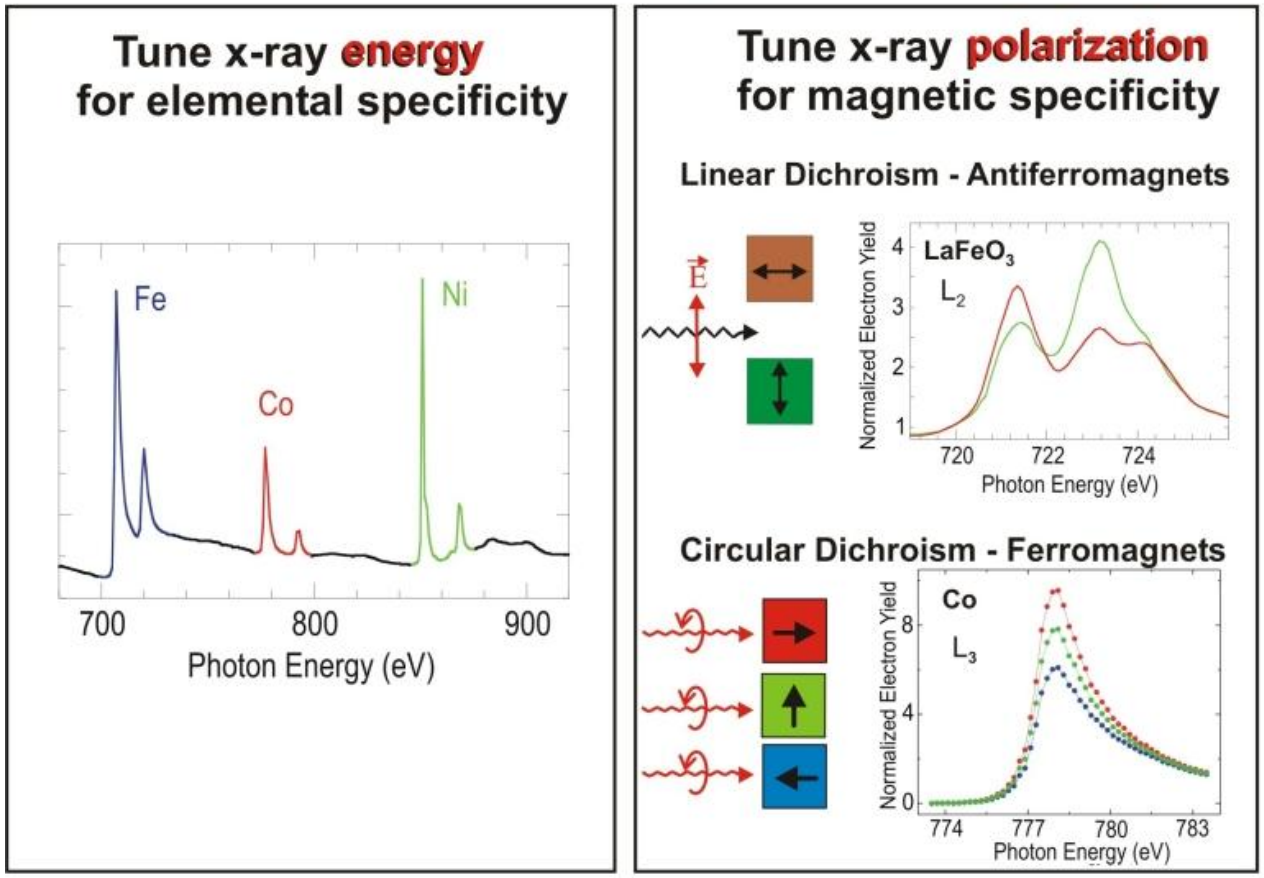

UFMG

LNLS

1. Tutorial: The concept of XMCD – Spin and Orbital Moments

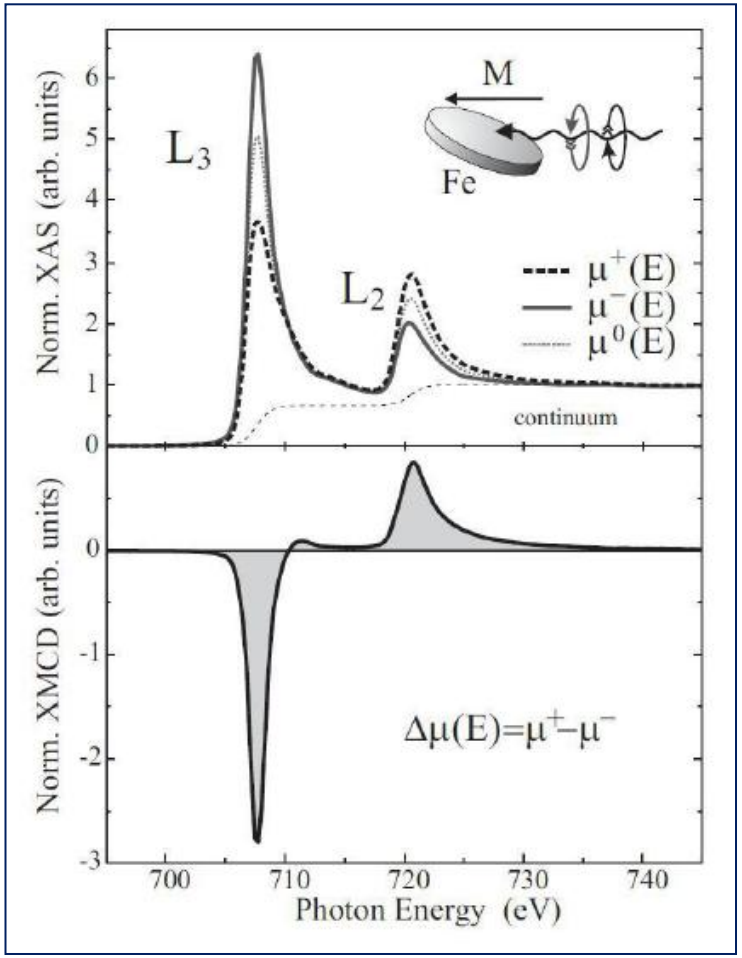

μ(E) - X-ray absorption for different polarizations

Δμ(E) = XMCD signal

Usually one inverts the magnetic field instead of changing polarizations

UFMG

LNLS

1. Tutorial: XMCD – Spin and Orbital Moments sum rules

μ(E) - X-ray absorption for different polarizations

$\Delta\mu(E) = \mu^{+}(E) - \mu^{-}(E)$ (XMCD signal)

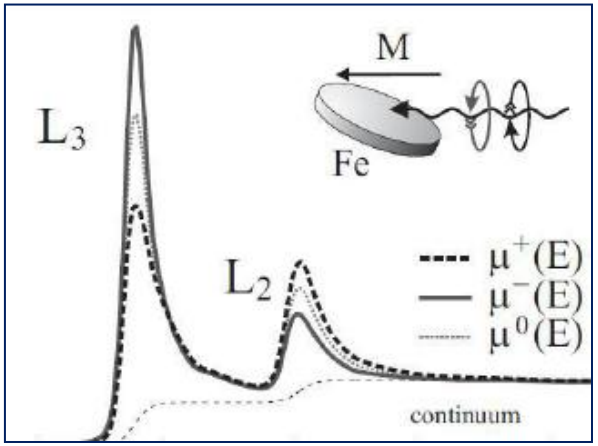

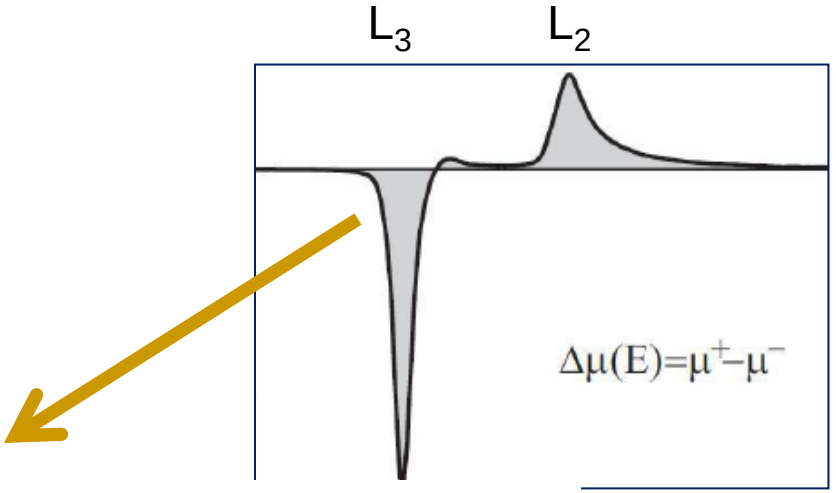

$$m_{spin} = -\frac{6\int_{L_3}(\mu_+ - \mu_-)dE - 4\int_{L_3+L_2}(\mu_+ - \mu_-)dE}{\int_{L_3+L_2}(\mu_+ + \mu_-)dE} * (10 - n_{3d})$$

$$m_{orb} = -\frac{4\int_{L_3}(\mu_+ - \mu_-)dE}{3\int_{L_2+L_3}(\mu_+ + \mu_-)dE} * (10 - n_{3d})$$

UFMG

LNLS

1. Tutorial: XMCD – Spin and Orbital Moments sum rules

$$m_{spin} = -\frac{6\int_{L3}(\mu_+ - \mu_-)dE - 4\int_{L3+L2}(\mu_+ - \mu_-)dE}{\int_{L3+L2}(\mu_+ + \mu_-)dE}(10 - n_{3d})(1 + \frac{7\langle T_z\rangle}{2\langle S_z\rangle})$$

$$m_{orb} = -\frac{4\int_{L3}(\mu_+ - \mu_-)dE}{3\int_{L3+L2}(\mu_+ + \mu_-)dE}(10 - n_{3d})$$

$$m_{orb}/m_{spin} = \frac{2\int_{L3+L2}(\mu_+ - \mu_-)dE}{9\int_{L3}(\mu_+ - \mu_-)dE - 6\int_{L3+L2}(\mu_+ - \mu_-)dE}$$

1. Tutorial: XMCD – Spin and Orbital Moments sum rules

C. T. Chen et al., Phys. Rev. Lett. 75, 152 (1995)

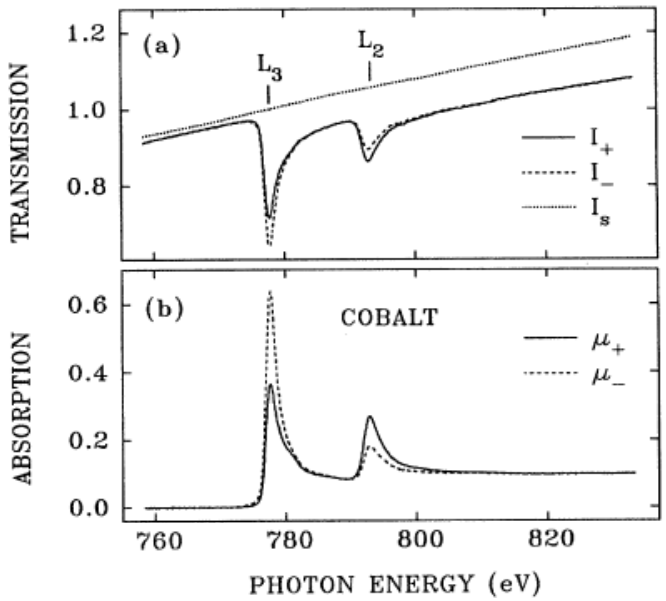

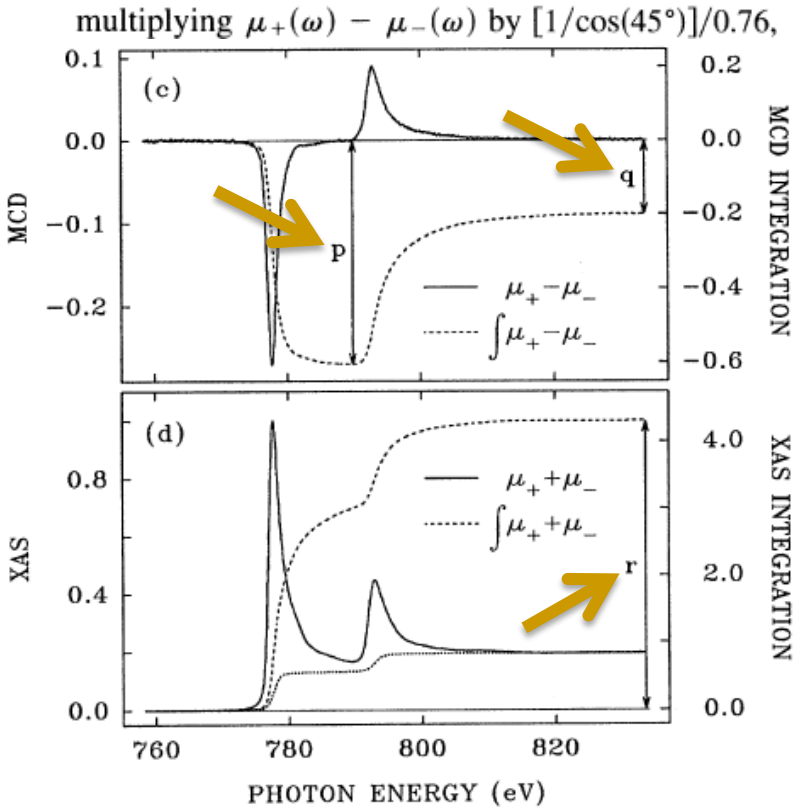

Theoretical papers:
B. T. Thole et al., Phys. Rev. Lett. 68, 1943 (1992)
P. Carra et al., Phys. Rev. Lett. 70, 694 (1993)

UFMG

LNLS

1. Tutorial: XMCD – Spin and Orbital Moments sum rules

VOLUME 75, NUMBER 1 PHYSICAL REVIEW LETTERS 3 JULY 1995

Experimental Confirmation of the X-Ray Magnetic Circular Dichroism Sum Rules for Iron and Cobalt

C. T. Chen,[1] Y. U. Idzerda,[2] H.-J. Lin,[1,*] N. V. Smith,[1,†] G. Meigs,[1] E. Chaban,[1]
G. H. Ho,[3,*] E. Pellegrin,[1] and F. Sette[1,‡]

[1]*AT&T Bell Laboratories, 600 Mountain Avenue, Murray Hill, New Jersey 07974*
[2]*Naval Research Laboratory, Washington, DC 20375*
[3]*Department of Physics, University of Pennsylvania, Philadelphia, Pennsylvania 19104*
(Received 12 May 1994; revised manuscript received 30 September 1994)

TABLE I. Orbital and spin magnetic moments of bcc Fe and hcp Co in units of μ_B/atom.

	Fe (bcc)			Co (hcp)		
	m_{orb}/m_{spin}	m_{orb}	m_{spin}	m_{orb}/m_{spin}	m_{orb}	m_{spin}
MCD and sum rules	0.043	0.085	1.98	0.095	0.154	1.62
Gyromagnetic ratio [16]	0.044	0.092	2.08	0.097	0.147	1.52
OP-LSDA [17]	0.042	0.091	2.19	0.089	0.140	1.57
OP-LSDA (with OP off) [17]	0.027	0.059	2.19	0.057	0.090	1.57
SPR-LMTO [10]	0.020	0.043	2.20	0.054	0.087	1.60
FLAPW [11]	0.023	0.050	2.16	0.045	0.071	1.58
MCD and sum rules (corrected)	0.043	0.086	1.98	0.099	0.153	1.55

UFMG

LNLS

2. Scientific cases: A. Anomalous Palladium magnetism in nanostructures

VOLUME 91, NUMBER 19 PHYSICAL REVIEW LETTERS week ending 7 NOVEMBER 2003

Surface Ferromagnetism of Pd Fine Particles

T. Shinohara* and T. Sato
Department of Applied Physics and Physico-Informatics, Faculty of Science and Technology, Keio University, Hiyoshi, Yokohama 223-8522, Japan

T. Taniyama
Department of Innovative and Engineered Materials, Tokyo Institute of Technology, Nagatsuta, Yokohama 226-8502, Japan
(Received 17 July 2003; published 4 November 2003)

We report clear evidence of the ferromagnetism of gas-evaporated Pd fine particles with a clean surface. The clean Pd particle is found to have a magnetic heterostructure: the surface of the particle is ferromagnetic and the rest is paramagnetic. The size dependence of the magnetic saturation component reveals that the ferromagnetic ordering occurs only on (100) facets of the particle and that the topmost two to five layers from the surface contribute to the ferromagnetism with a magnetic moment of $(0.75 \pm 0.31)\mu_B$/atom.

DOI: 10.1103/PhysRevLett.91.197201 PACS numbers: 75.50.Gg, 75.50.Tt, 75.70.Rf, 75.75.+a

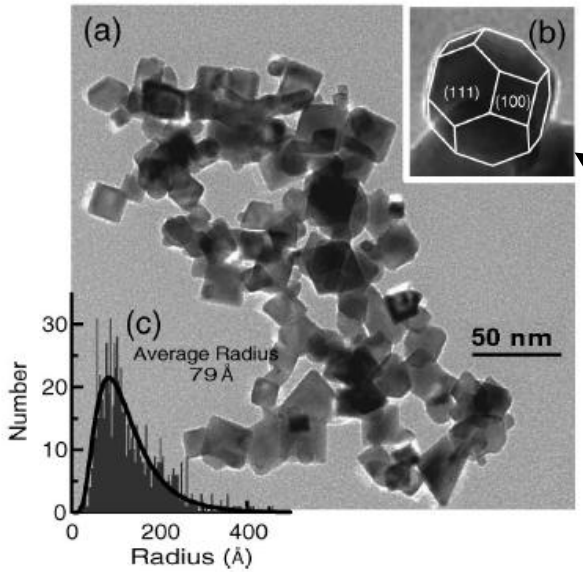

Techniques:
DRX,TEM, SQUID

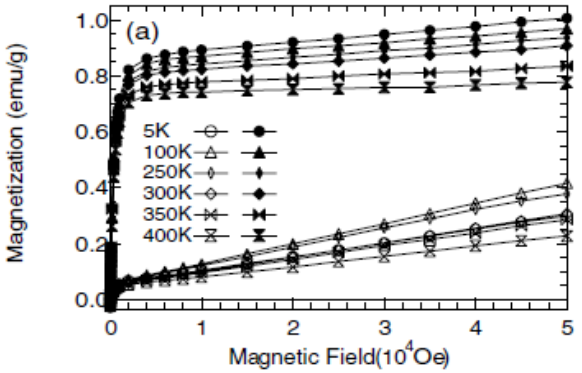

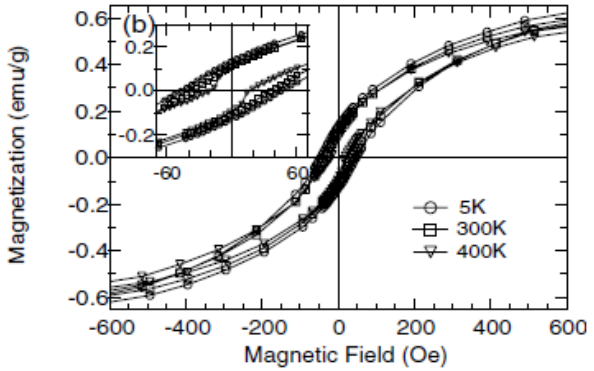

Ferromagnetism on the facets!
(111)
(100)

2. Scientific cases: A. Anomalous Palladium magnetism in nanostructures

VOLUME 91, NUMBER 23 PHYSICAL REVIEW LETTERS week ending 5 DECEMBER 2003

Ferromagnetism in fcc Twinned 2.4 nm Size Pd Nanoparticles

B. Sampedro,[1,2] P. Crespo,[1,2] A. Hernando,[1,2] R. Litrán,[3] J. C. Sánchez López,[3] C. López Cartes,[3] A. Fernandez,[3] J. Ramírez,[4] J. González Calbet,[1,4] and M. Vallet[1,5]

[1]*Instituto de Magnetismo Aplicado, "Salvador Velayos," UCM, RENFE, CSIC, Las Rozas, P.O. Box 155, Madrid 28230, Spain*
[2]*Departamento de Física de Materiales, UCM, Madrid 28040, Spain*
[3]*Instituto de Ciencias de Materiales de Sevilla (ICMSE), Centro Mixto CSIC-UNIV, Sevilla 41092, Spain*
[4]*Departamento de Química Inorgánica, Facultad de Química, UCM, Madrid 28040, Spain*
[5]*Departamento de Química Inorgánica, Facultad de Farmacia, UCM, Madrid 28040, Spain*
(Received 24 July 2003; published 4 December 2003)

The onset of ferromagnetism has been experimentally observed in small Pd particles of average diameter 2.4 nm. High-resolution studies reveal that a high percentage of the fcc particle exhibits single and multiple twinning boundaries. The spontaneous magnetization close to 0.02 emu/g seems to indicate that only a small fraction of atoms holds a permanent magnetic moment and contributes to ferromagnetism. The possible origin of ferromagnetism is briefly discussed according to different models recently reported.

DOI: 10.1103/PhysRevLett.91.237203 PACS numbers: 75.50.Cc, 75.50.Tt, 75.70.Cn

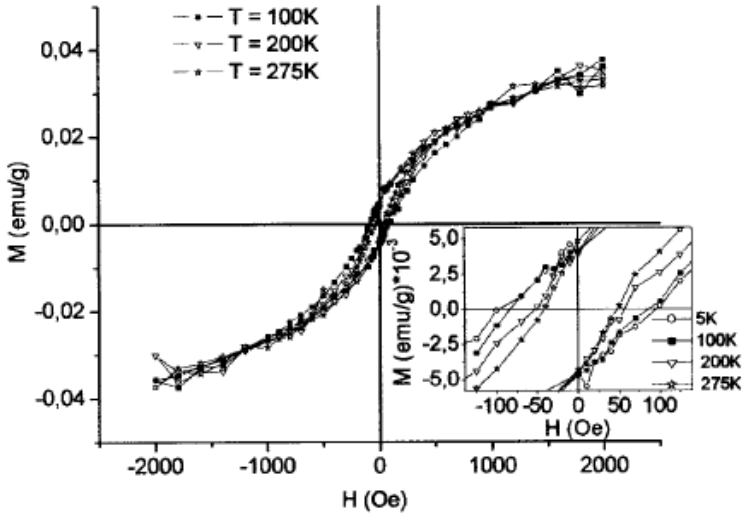

Techniques:
HRTEM, SQUID

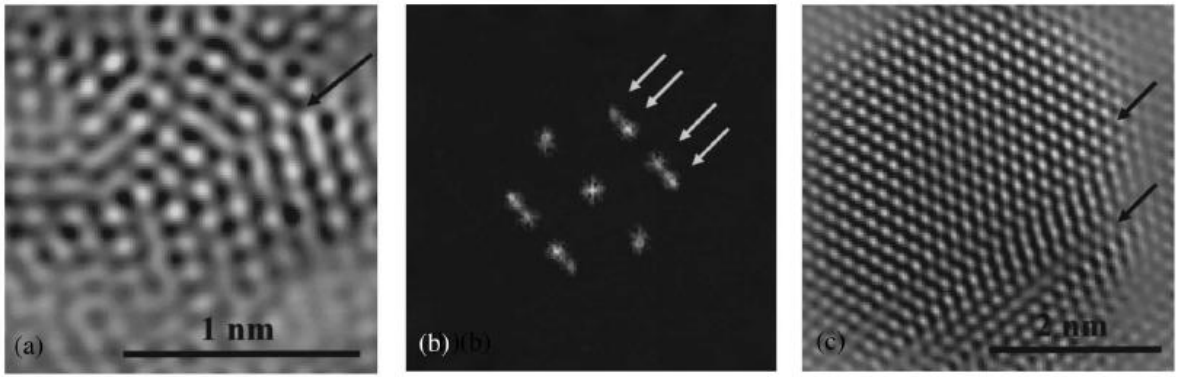

Ferromagnetism due to defects (stacking faults)!

2A. Palladium magnetism: Stoner Criterion for Magnetism of Conduction Electrons

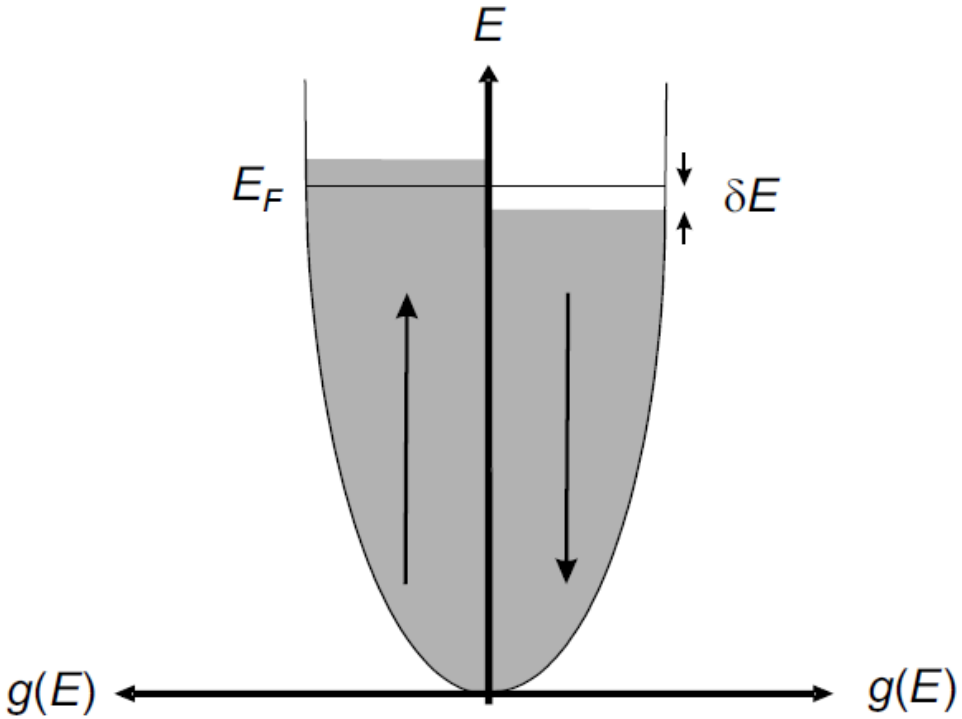

$$\Delta E_{\text{kin}} = \frac{1}{2} g(E_F)(\delta E)^2$$

$$\Delta E_{\text{pot}} = -\frac{1}{2} U \cdot (g(E_F)\delta E)^2$$

$$U = \mu_0 \mu_B^2 \lambda$$

$$\Delta E = \Delta E_{\text{kin}} + \Delta E_{\text{pot}}$$

$$= \frac{1}{2} g(E_F)(\delta E)^2 \left(1 - U \cdot g(E_F)\right)$$

$\Delta E < 0$ → Energetically favorable

→ Stoner Criterion: $U \cdot g(E_F) \geq 1$

2A. Palladium magnetism: Stoner Criterion for Magnetism of Conduction Electrons

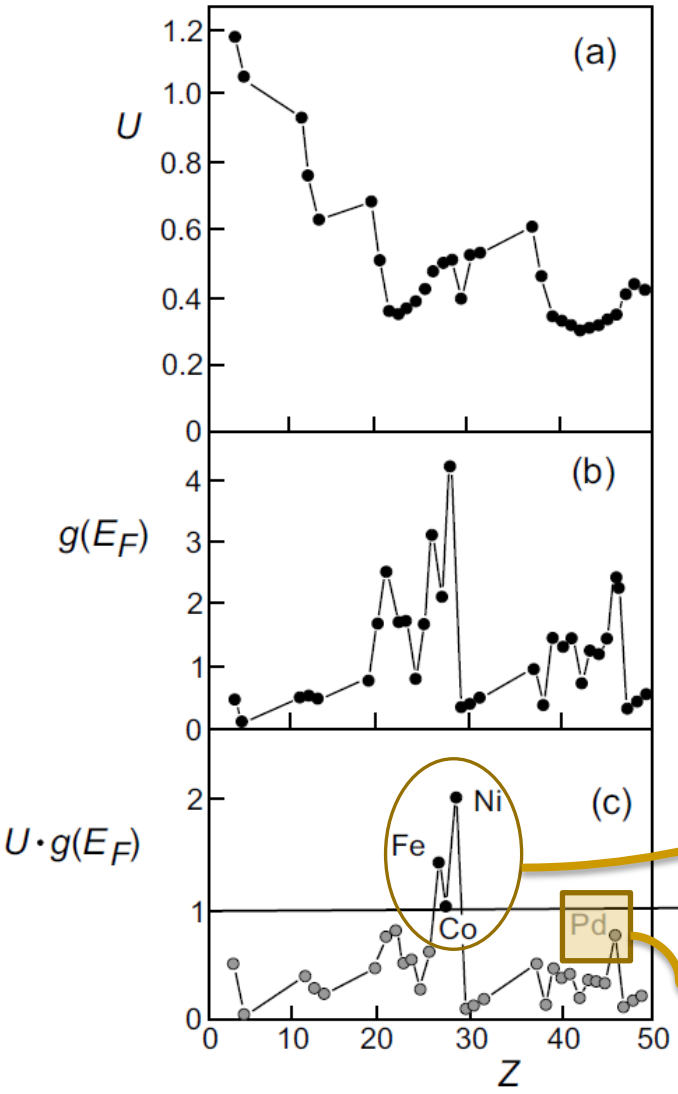

$$U \cdot g(E_F) \geq 1$$

DOS at the Fermi Energy

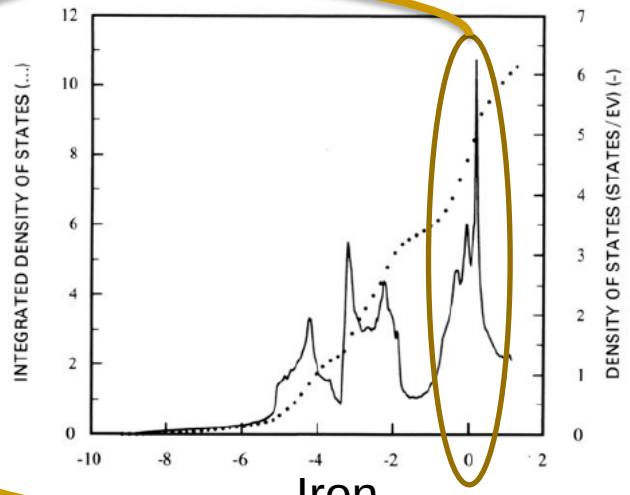

Iron

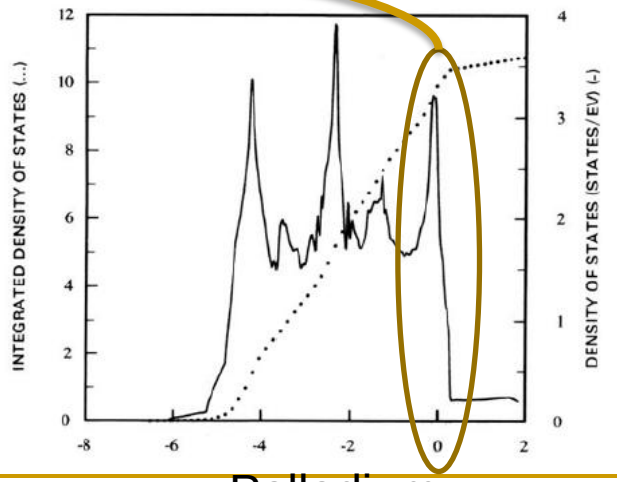

Palladium

Almost...

2A. Observation of Ferromagnetism in PdCo nanoparticles encapsulated in Carbon Nanotubes

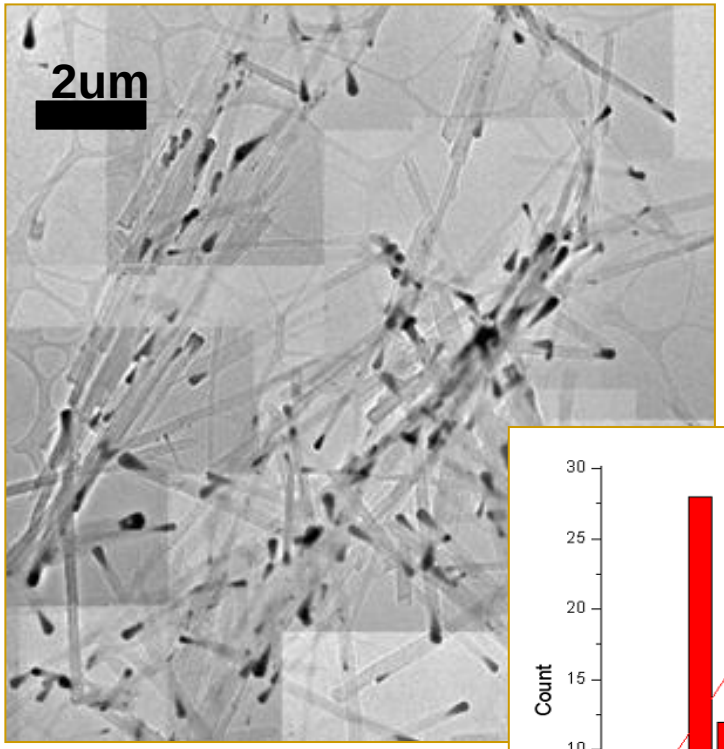

Técnica de crescimento: Deposição Química na Fase Vapor Assistida por Plasma – PECVD.

- Alto controle;
- Alinhamento vertical.

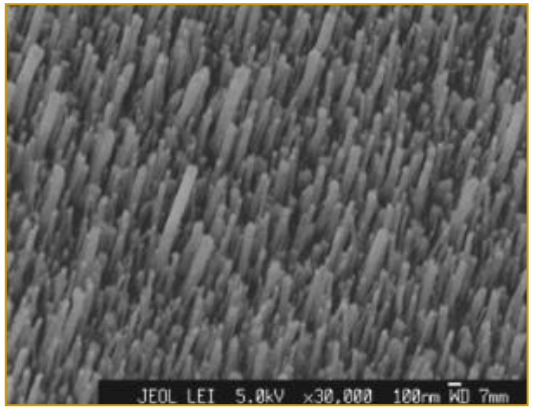

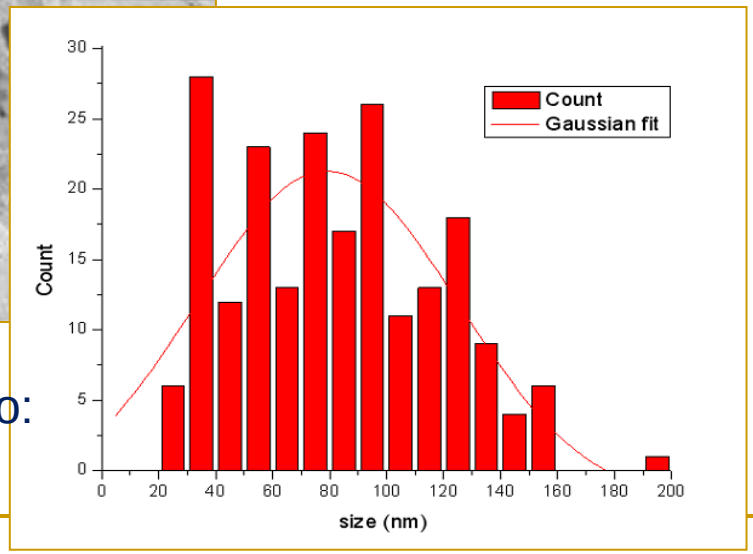

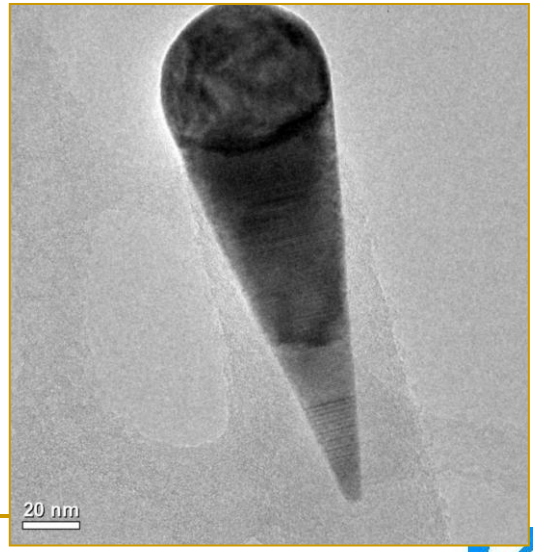

Distribuição de tamanho:
Diâmetro = (79 ± 30)nm

2A. Observation of Ferromagnetism in PdCo em nanoparticles encapsulated in Carbon Nanotubes

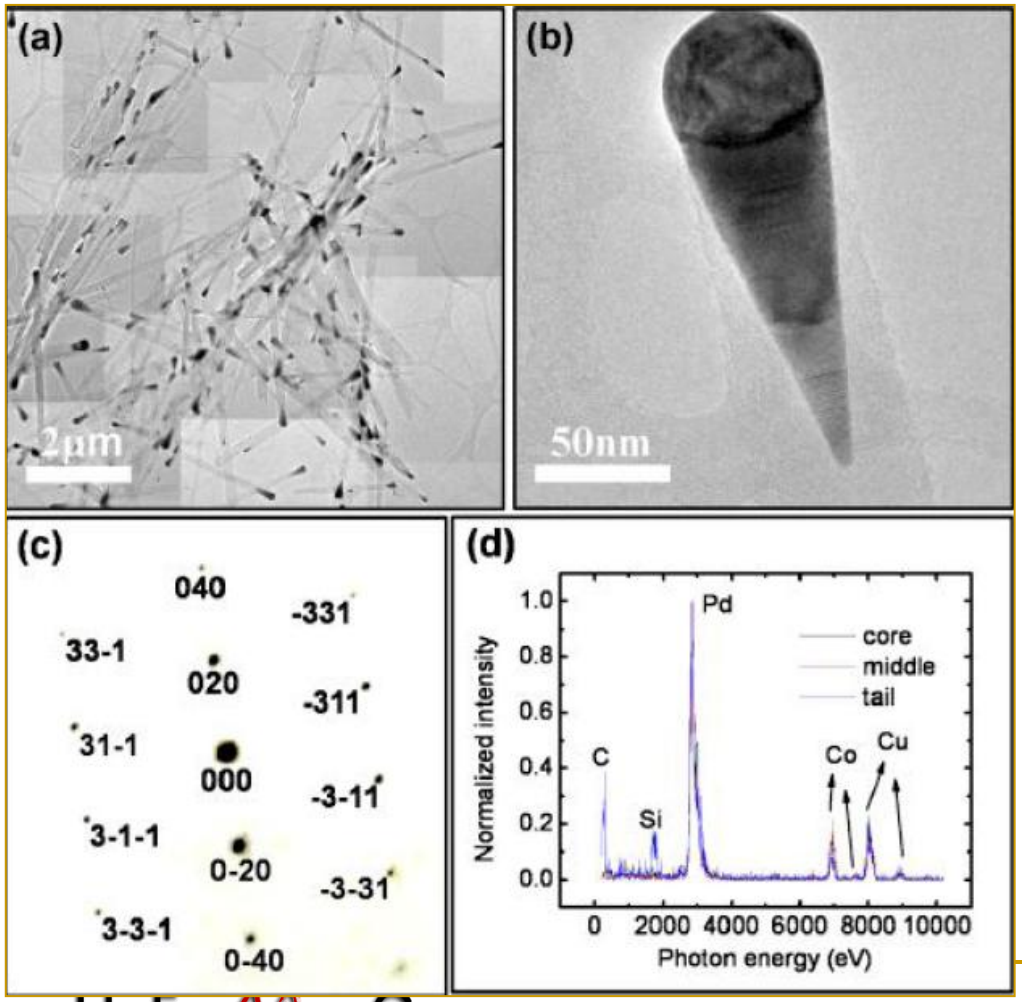

Microscopia Eletrônica de Transmissão (TEM)

Homogeneidade da amostra;

Anisotropia de forma das partículas;

Estrutura cristalina: PdCo (fcc) próxima a do Paládio *bulk*.

Concentração de Pd em relação ao Co ao longo da partícula é aproximadamente constante

UFMG

LNLS

2A. Observation of Ferromagnetism in PdCo em nanoparticles encapsulated in Carbon Nanotubes

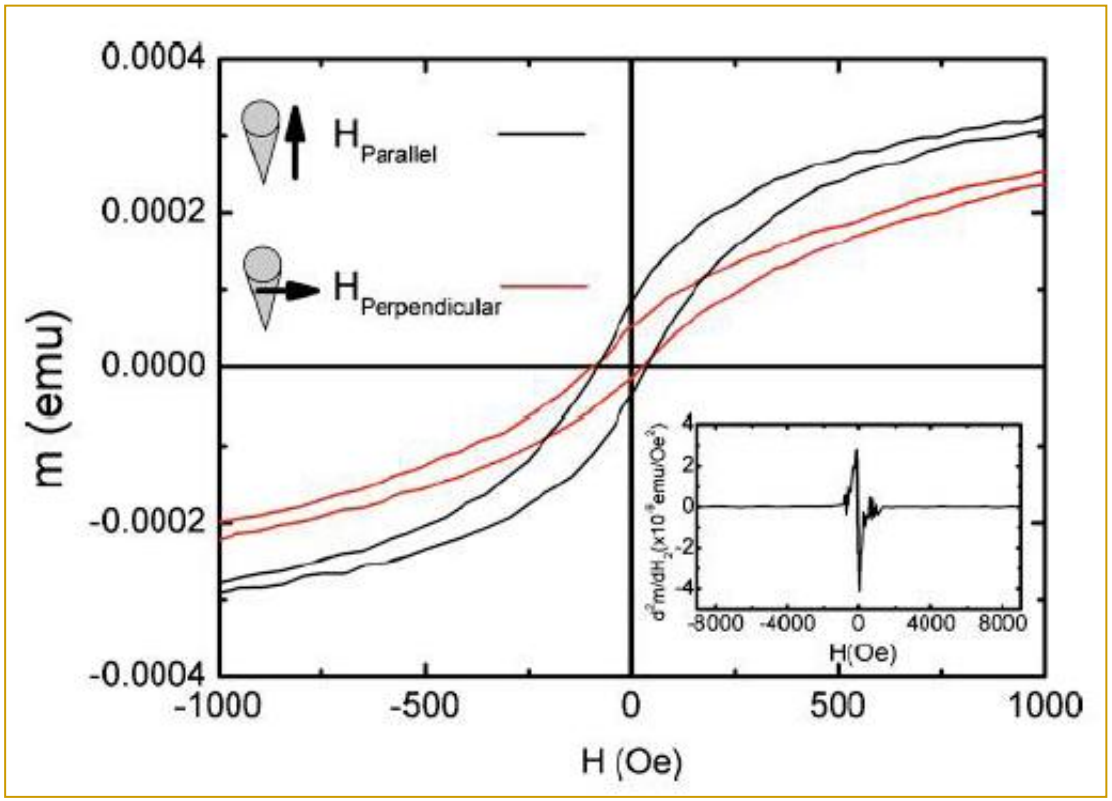

Magnetometria de amostra vibrante (VSM)

Comportamento magnético global da amostra;

Temperatura ambiente;

Campo de saturação: 1500 Oe

Anisotropia magnética uniaxial:
- eixo duro: H perpendicular;
- eixo fácil: H longitudinal.

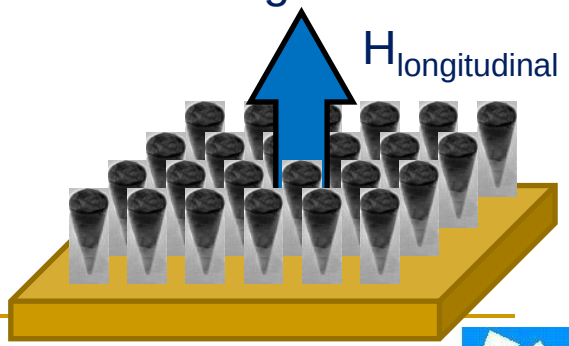

UFMG

LNLS

2A. A. Observation of Ferromagnetism in PdCo em nanoparticles encapsulated in Carbon Nanotubes

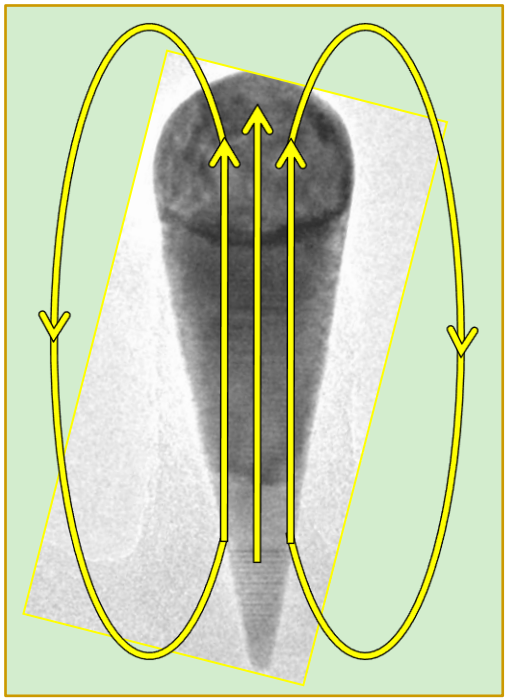

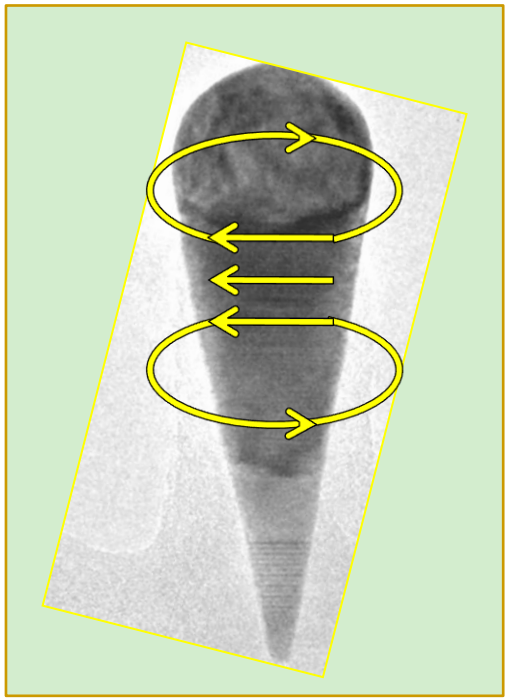

Magnetometria de amostra vibrante (VSM)

Comportamento magnético global da amostra;

Temperatura ambiente;

Campo de saturação: 1500 Oe

Anisotropia magnética uniaxial:
- eixo duro: H perpendicular;
- eixo fácil: H longitudinal.

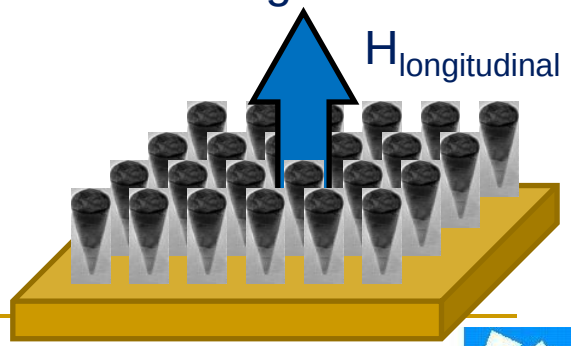

UFMG

LNLS

2A. Observation of Ferromagnetism in PdCo em nanoparticles encapsulated in Carbon Nanotubes

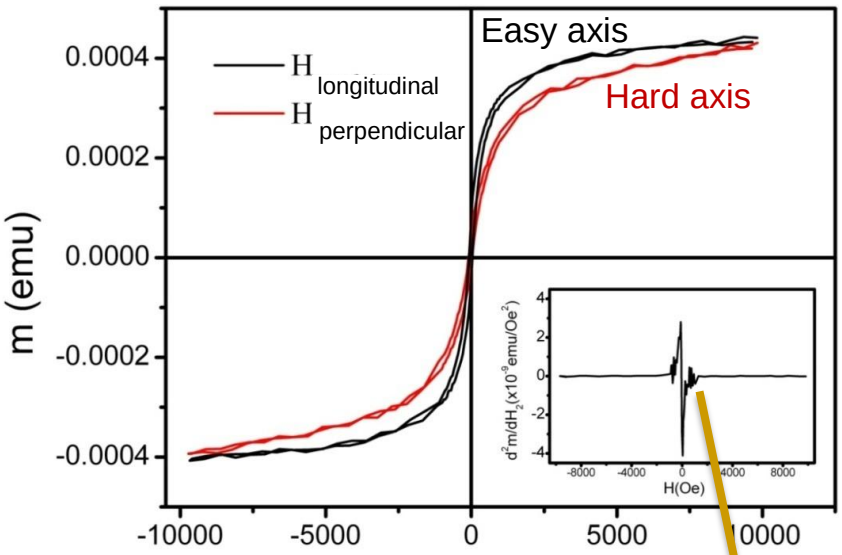

Longitudinal: easy axis

Perpendicular: hard axis

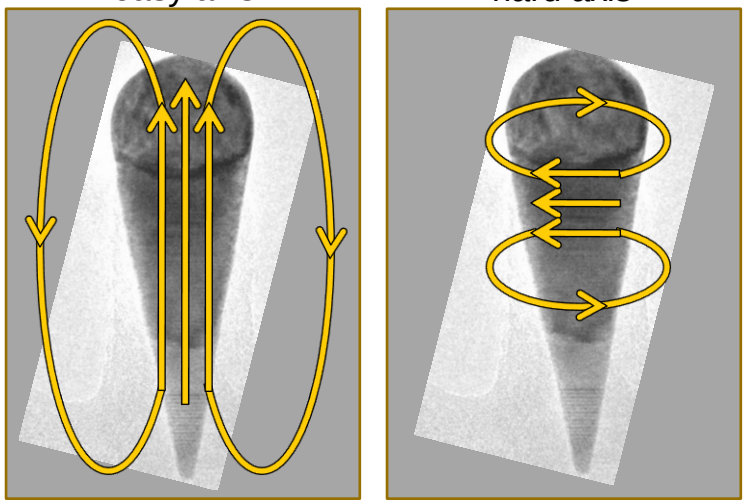

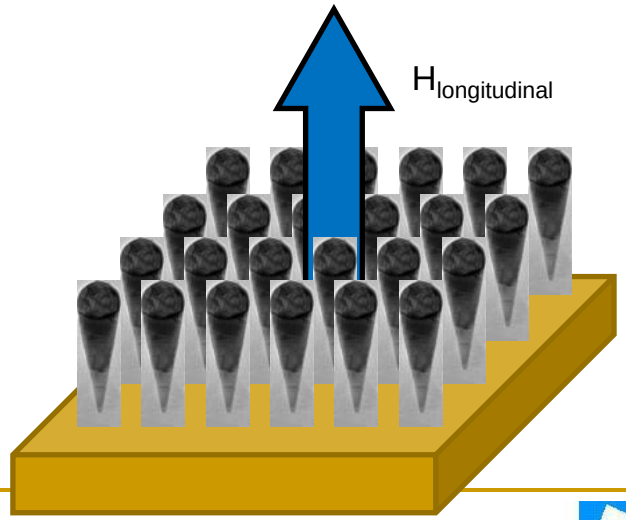

Second derivative:
Removing paramagnetic signal

Hc = 150 Oe

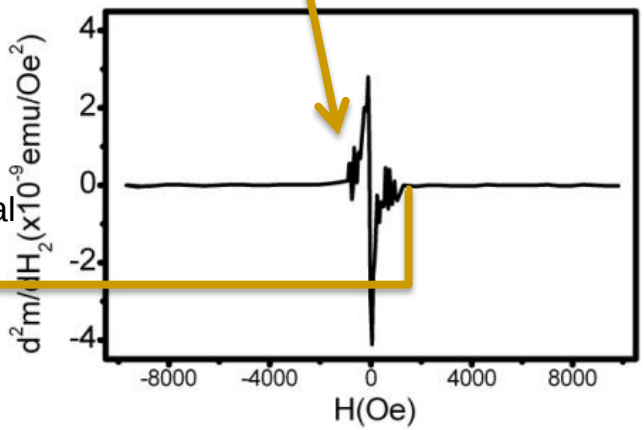

2A. Observation of Ferromagnetism in PdCo em nanoparticles encapsulated in Carbon Nanotubes

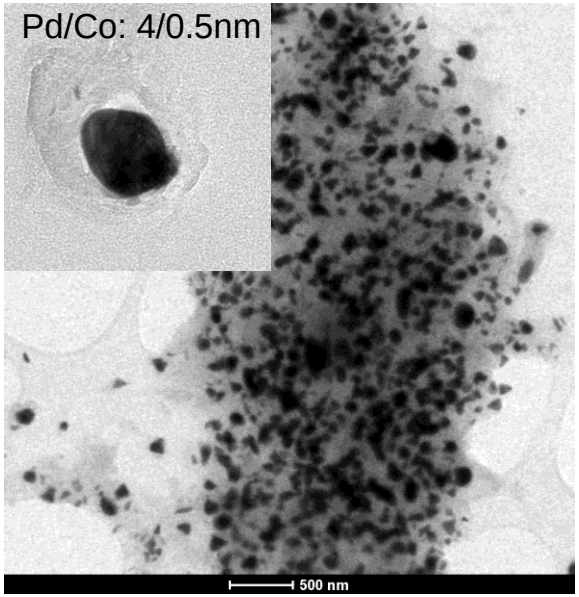

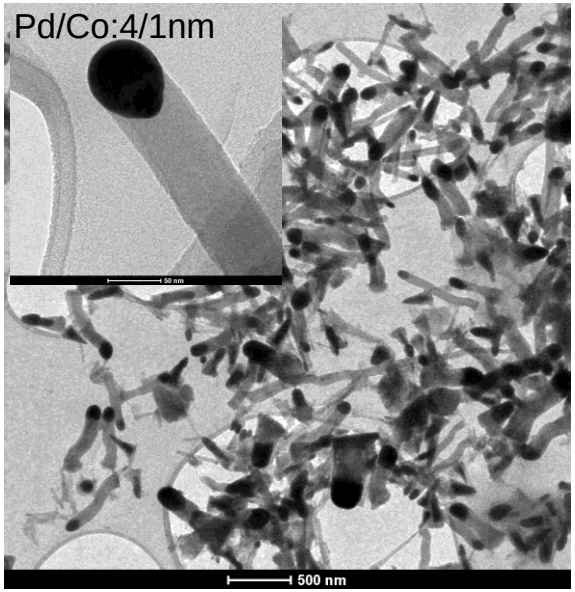

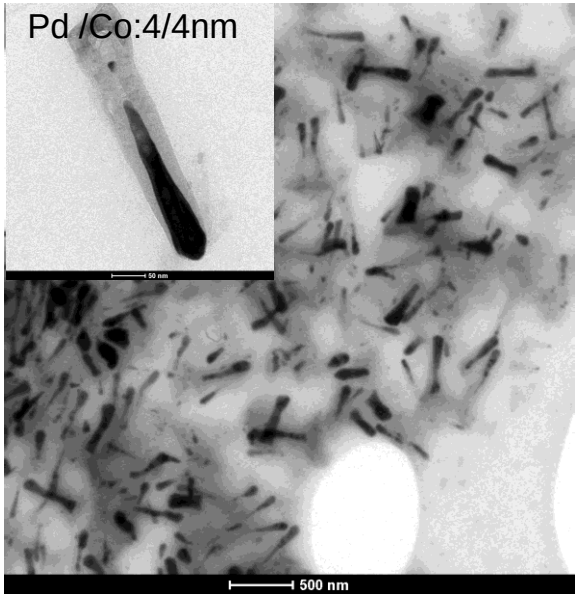

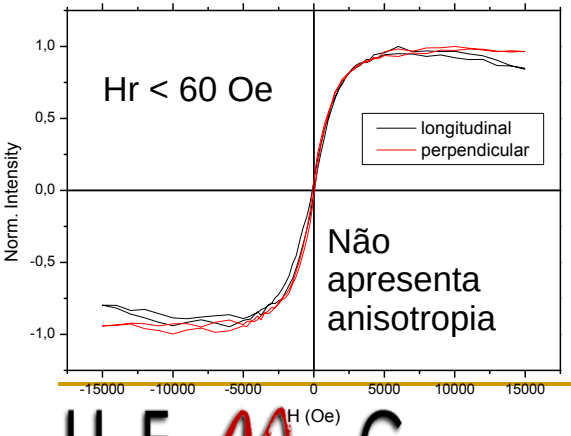

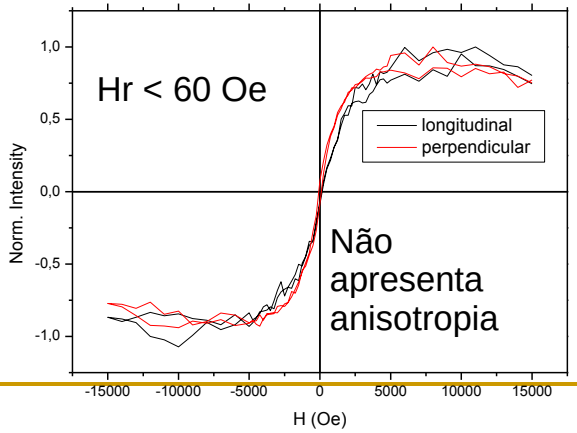

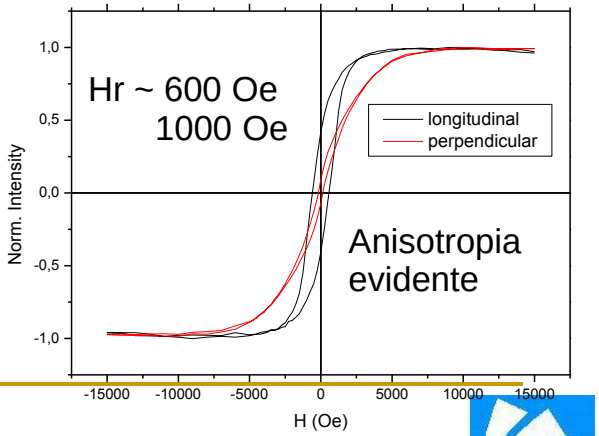

UFMG

LNLS

2A. X-ray magnetic circular dichroism of PdCo nanoparticles

XMCD at LNLS

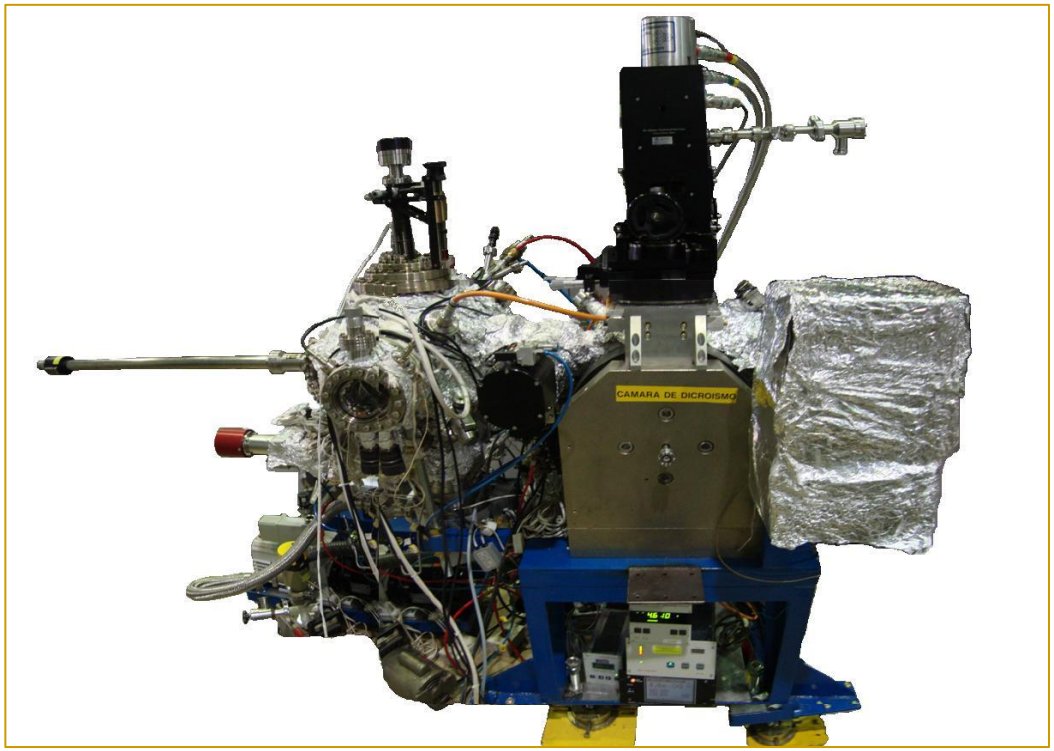

Informação magnética com informação química-estrutural!

Temperatura ambiente;

LNLS, linhas de luz: bordas L_2 e L_3
- Co – PGM (100-1000ev);
- Pd – SXS (1000-3000eV);

Campo magnético aplicado:
- ~10000 Oe (1 T)
- <6x o necessário

UFMG

LNLS

2A. Observation of Ferromagnetism in PdCo em nanoparticles encapsulated in Carbon Nanotubes

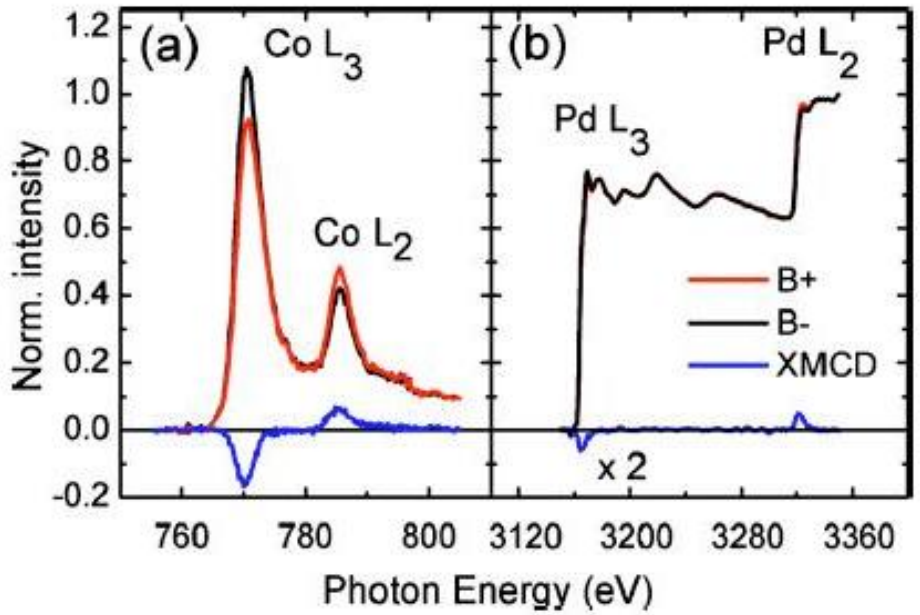

Dicroísmo Circular Magnético de Raios-X (XMCD)

Cobalto:

$$m_{orb}/m_{spin} = (0,12 \pm 0,05)$$

Paládio:

$$m_{orb}/m_{spin} = (0,07 \pm 0,05)$$

Cobalto bulk: 0,099

APPLIED PHYSICS LETTERS **96**, 253114 (2010)

Observation of ferromagnetism in PdCo alloy nanoparticles encapsulated in carbon nanotubes

Daniel Bretas Roa,[1] Ingrid David Barcelos,[1] Abner de Siervo,[2,3] Kleber Roberto Pirota,[2] Rodrigo Gribel Lacerda,[1] and Rogério Magalhães-Paniago[1,a)]
[1]*Departamento de Física, Universidade Federal de Minas Gerais, 30123-970 Belo Horizonte, Brazil*
[2]*Instituto de Física Gleb Wataghin, Universidade Estadual de Campinas, 13083-970 Campinas, Brazil*
[3]*Laboratório Nacional de Luz Síncrotron, 13084-971 Campinas, Brazil*

UFMG

LNLS

2. Scientific cases: B. Room temperature observation of orbital momentum enhancement of Co nanoclusters grown on Au(110)

Low dimensional systems (nanoparticles, clusters, 1d systems) exhibit anomalous magnetic behavior)

Science AAAS

Giant Magnetic Anisotropy of Single Cobalt Atoms and Nanoparticles
P. Gambardella, *et al.*
Science **300**, 1130 (2003);
DOI: 10.1126/science.1082857

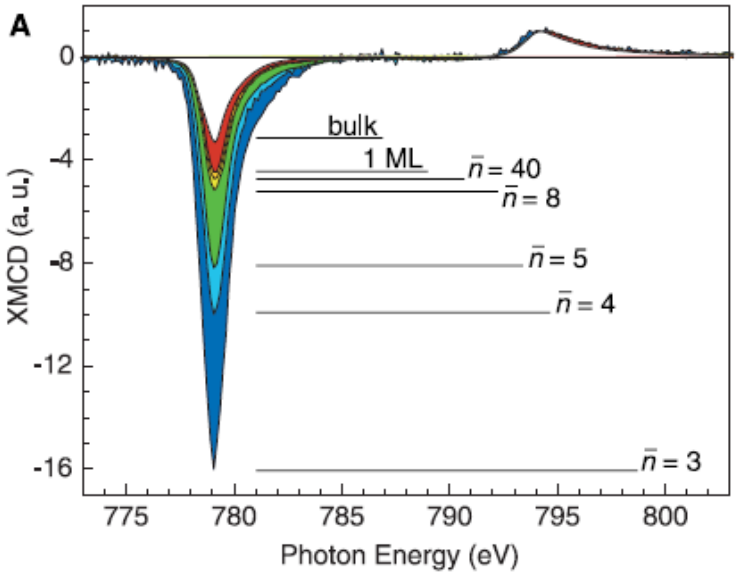

Techniques:

STM
(for size determination)

SQUID
(for magnetism)

XMCD
(orbital and spin momentum)

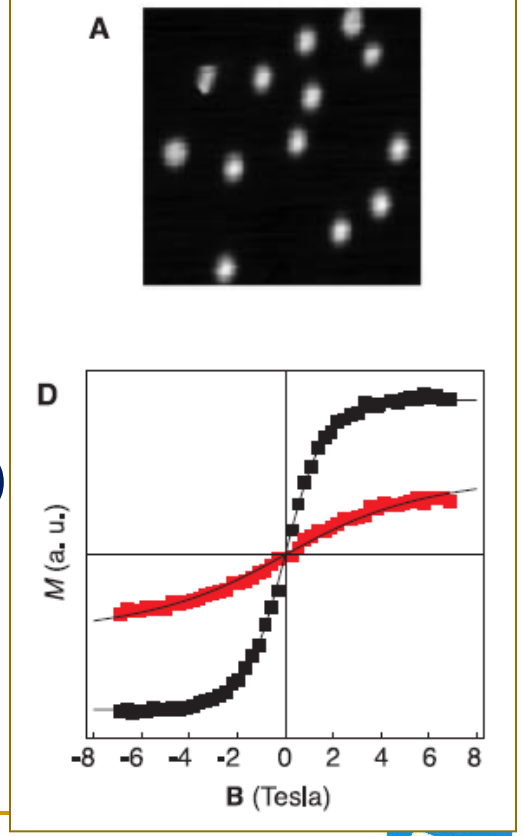

UFMG 5 Kelvin, 8 Tesla!!!

LNLS

XMCD at LNLS
New Beamline PGM

EPU-type Undulator beamline
VLS PGM monochromator
Polarized soft-X-rays
Energy = 100-1100eV

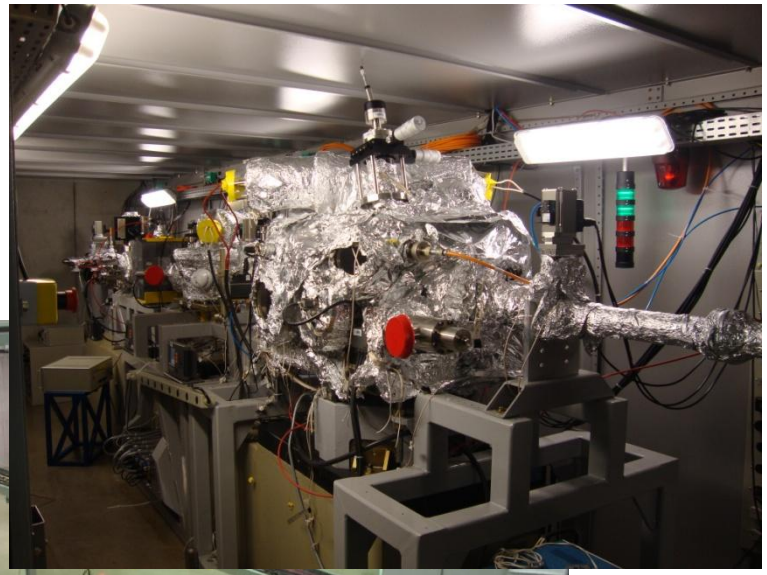

Applications:
X-ray magnetic circular dichroism
X-ray photoelectron Difraction
X-ray photoelectron Spectroscopy
Electron spectroscopy of liquids
Among others...

UFMG

LNLS

Test experiment: Magnetism of Cobalt nanoparticles grown on Au (110)

Preparation of Au(110) surface (2x1) reconstruction observed by low-energy electron diffraction)

Surface prepared by

1.5 KeV Ar+ sputtering, 400º C annealing , P_{base} =2 x 10^{-10} mBar

Asymmetric deposition of Cobalt

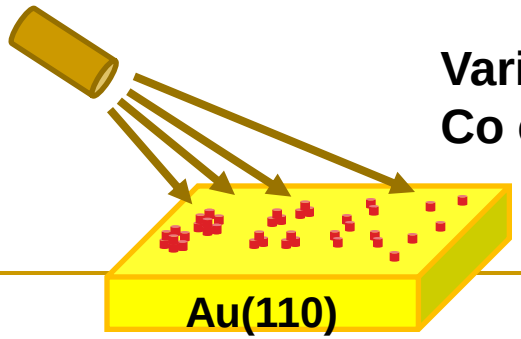

UFMG

LNLS

Preparation experiment at DF-UFMG:

STM and LEED of Au(110) and 4 ml Co/Au(110)

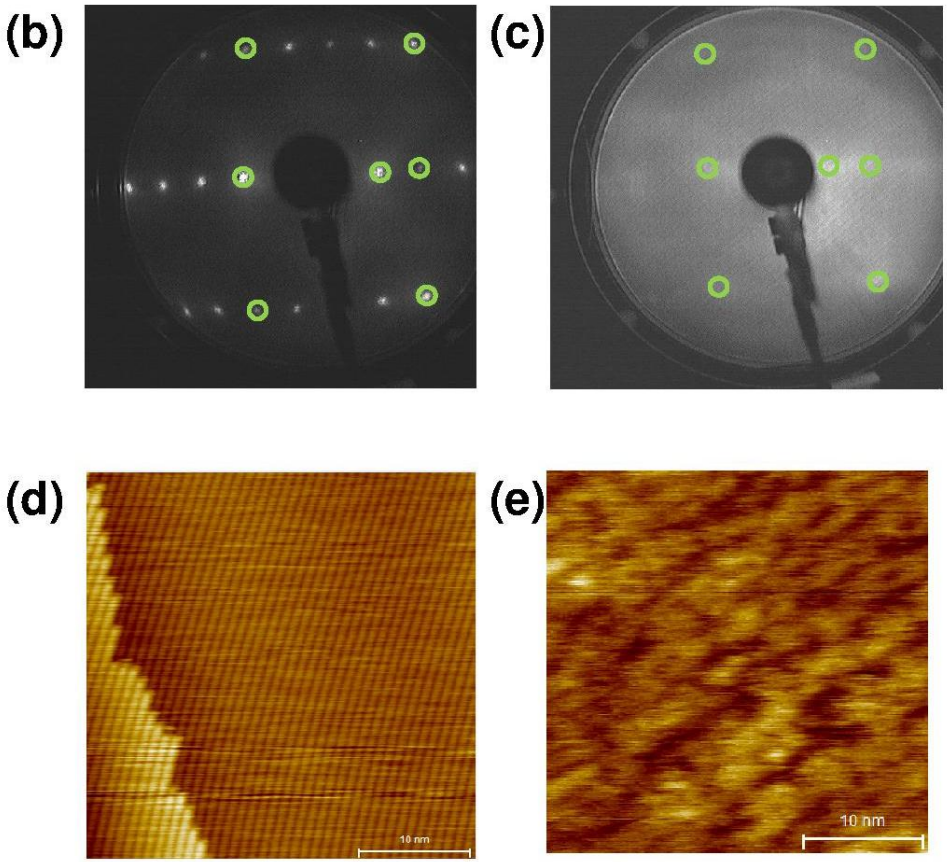

XMCD of Cobalt nanoparticles grown on Au (110)

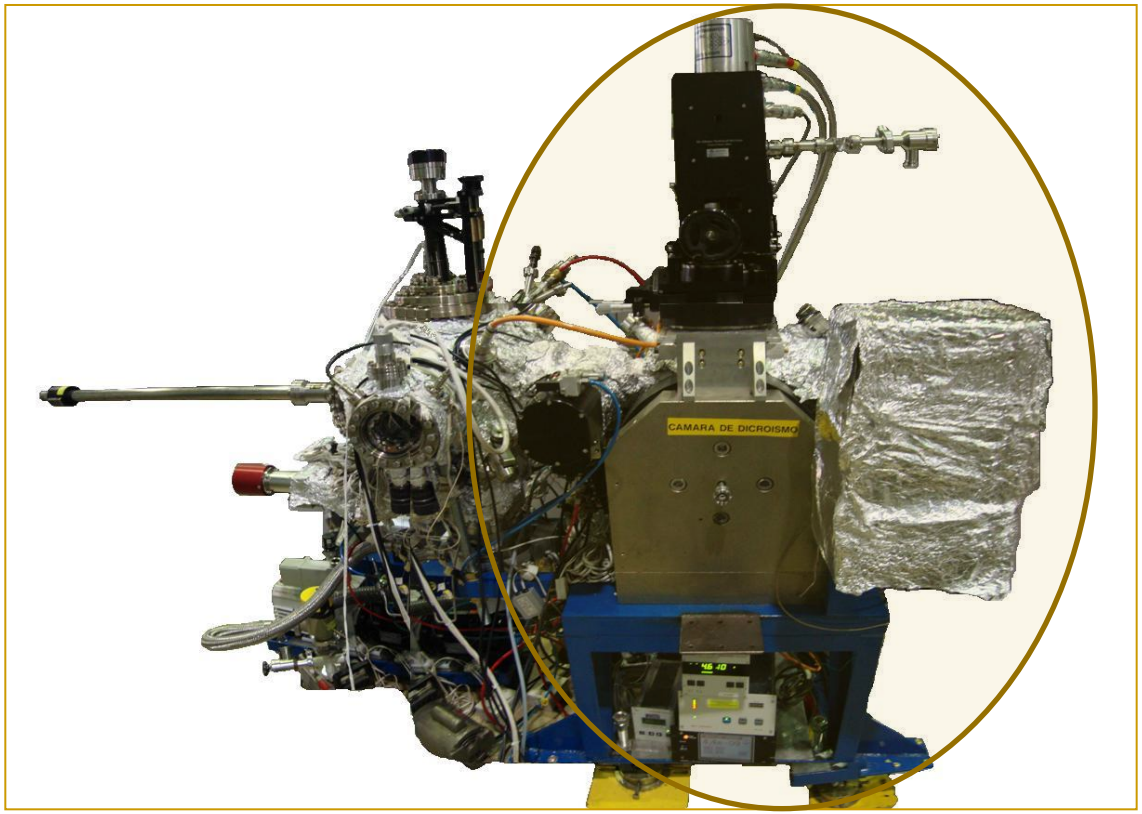

First measurement of systems of low dimensionality
Room temperature
Applied magnetic field 1.6 Tesla

Beamline PGM -LNLS,
Cobalt L_2 e L_3
Edges
PGM (200-1000ev);

UFMG

LNLS

X-ray absorption spectroscopy of Cobalt nanoparticles grown on Au (110)

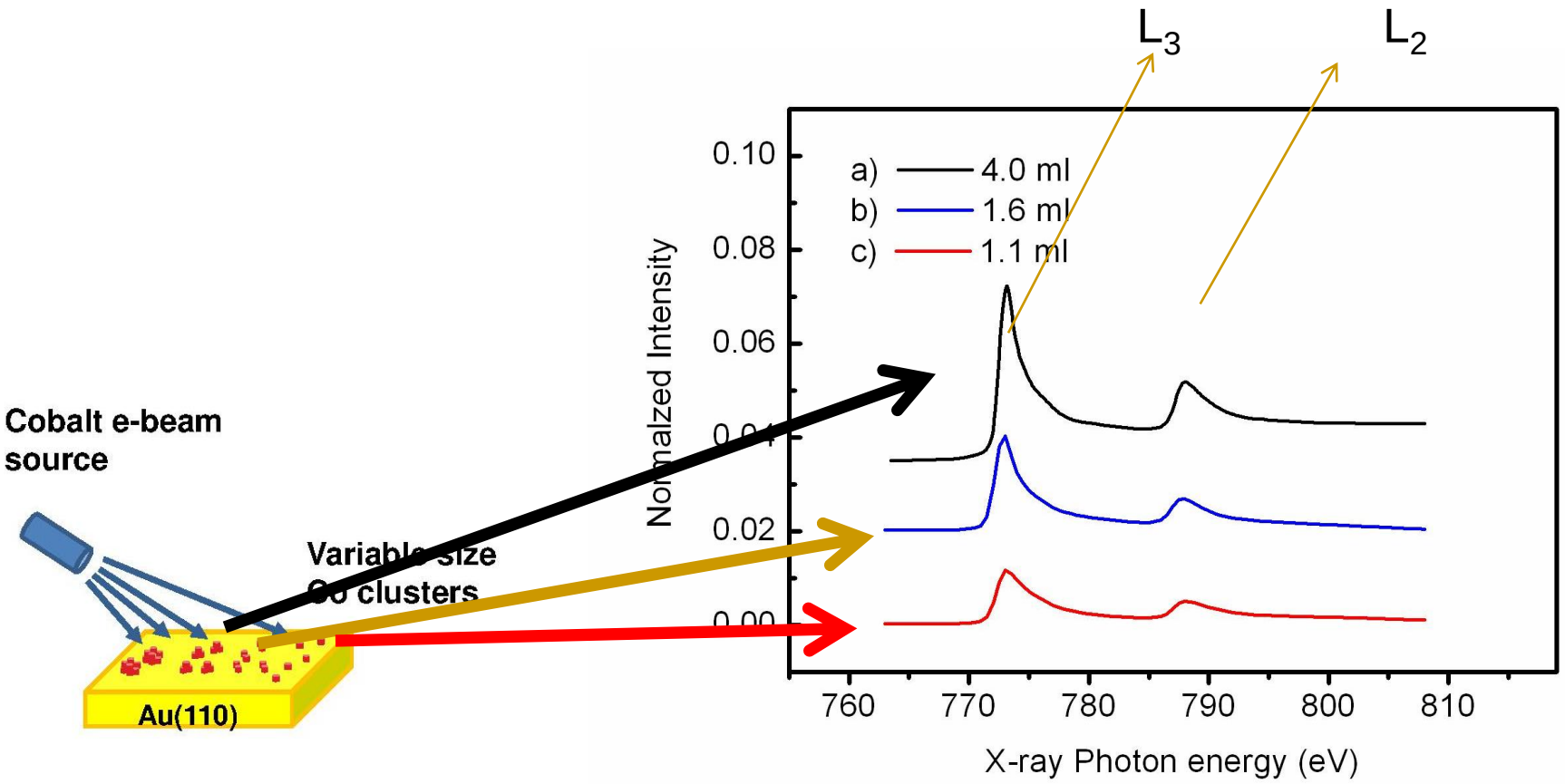

UFMG

LNLS

XMCD of Cobalt nanoparticles grown on Au (110)

The equivalent of 4 monolayers of Cobalt were deposited

Dichroism is evident

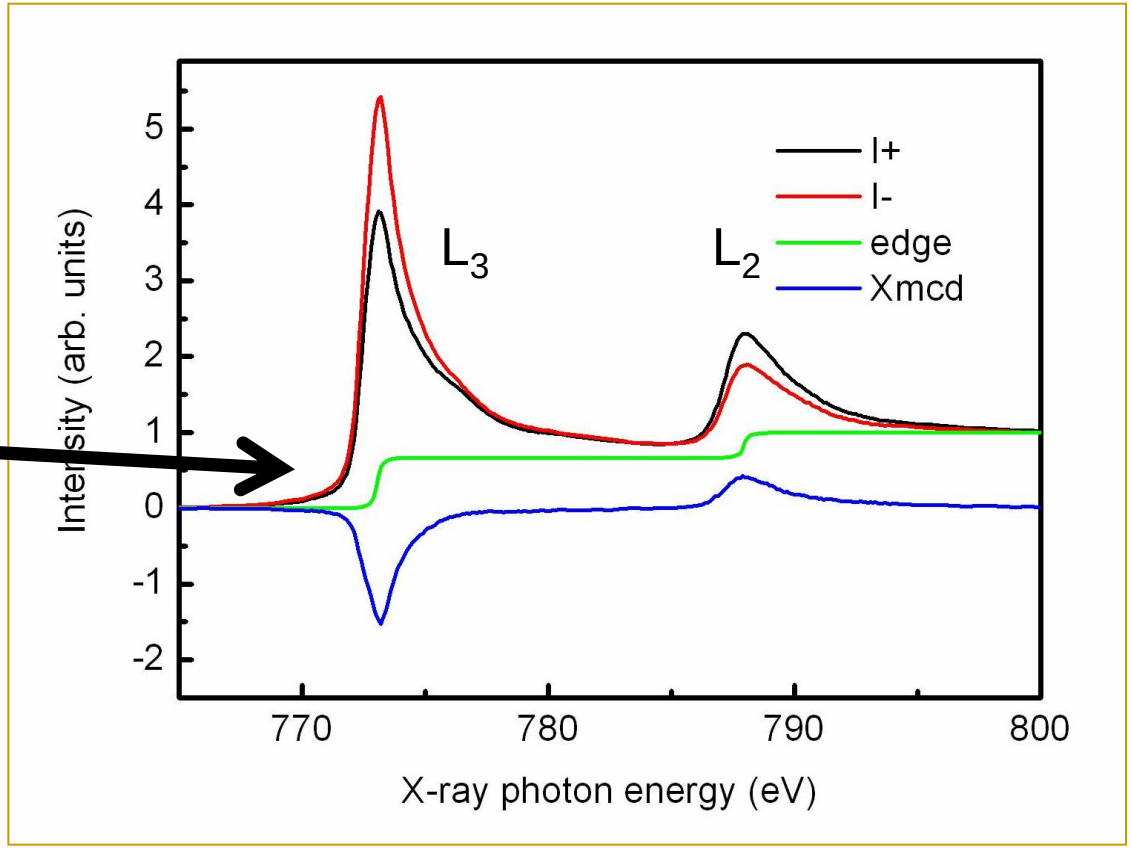

Determination of orbital moments is possible if magnetization is not saturated

$$m_{spin} = -\frac{6\int_{L_3}(\mu_+ - \mu_-)dE - 4\int_{L_3+L_2}(\mu_+ - \mu_-)dE}{\int_{L_3+L_2}(\mu_+ + \mu_-)dE} * (10 - n_{3d}) \quad \frac{1}{Pol \text{ x } \cos\theta} = 2.14\ \mu_B$$

$$m_{orb} = -\frac{4\int_{L_3}(\mu_+ - \mu_-)dE}{3\int_{L_2+L_3}(\mu_+ + \mu_-)dE} * (10 - n_{3d}) \quad \frac{1}{Pol \text{ x } \cos\theta} \qquad Pol = 0.78$$

Determination of θ using
m_{spin} = 2.14 μ_B

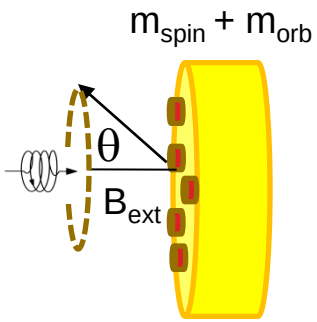

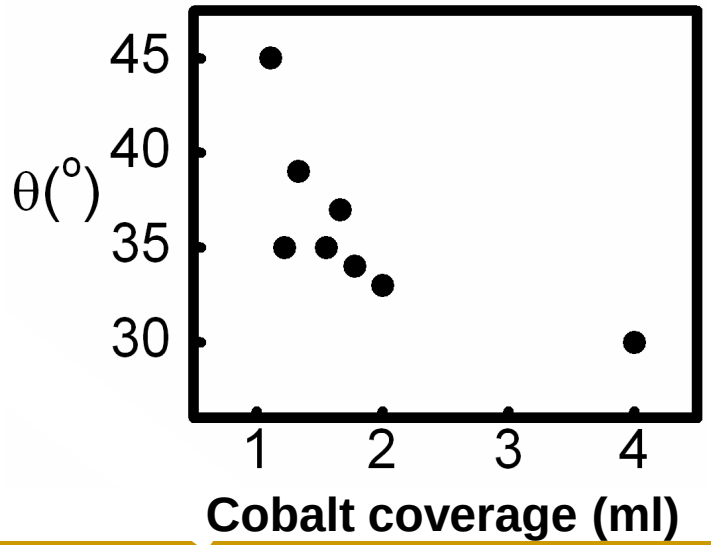

B_{ext} =1.6Tesla T=300K

Determination of orbital and spin moments is not possible if magnetization is not saturated

Low temperature (5Kelvin)

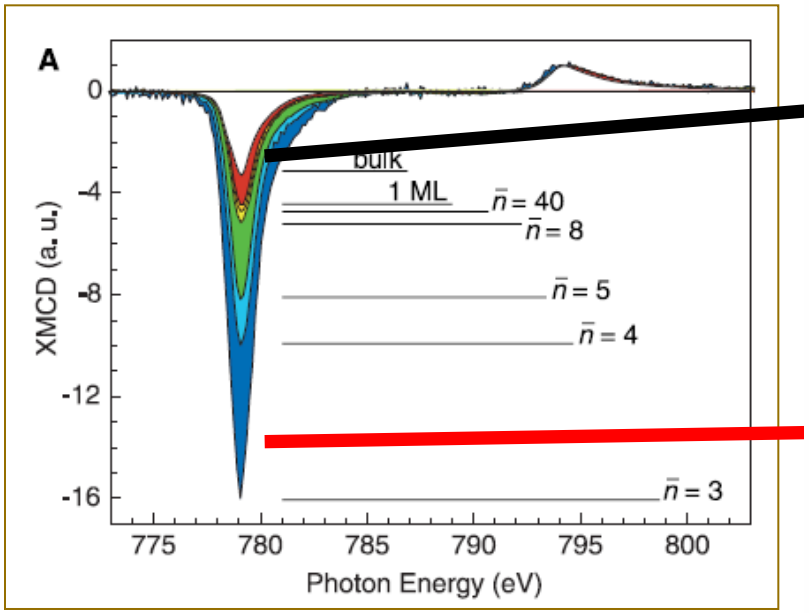

Room temperature (300Kelvin)

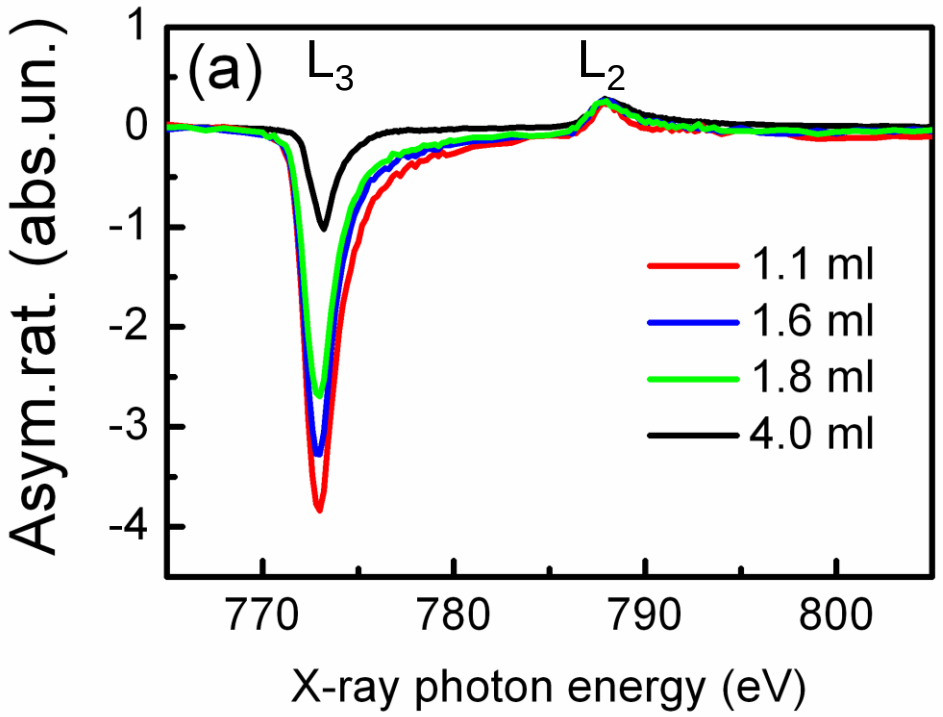

UFMG

LNLS

Large orbital momentum of Cobalt nanoparticles

m_L (bulk Co) → 0.2

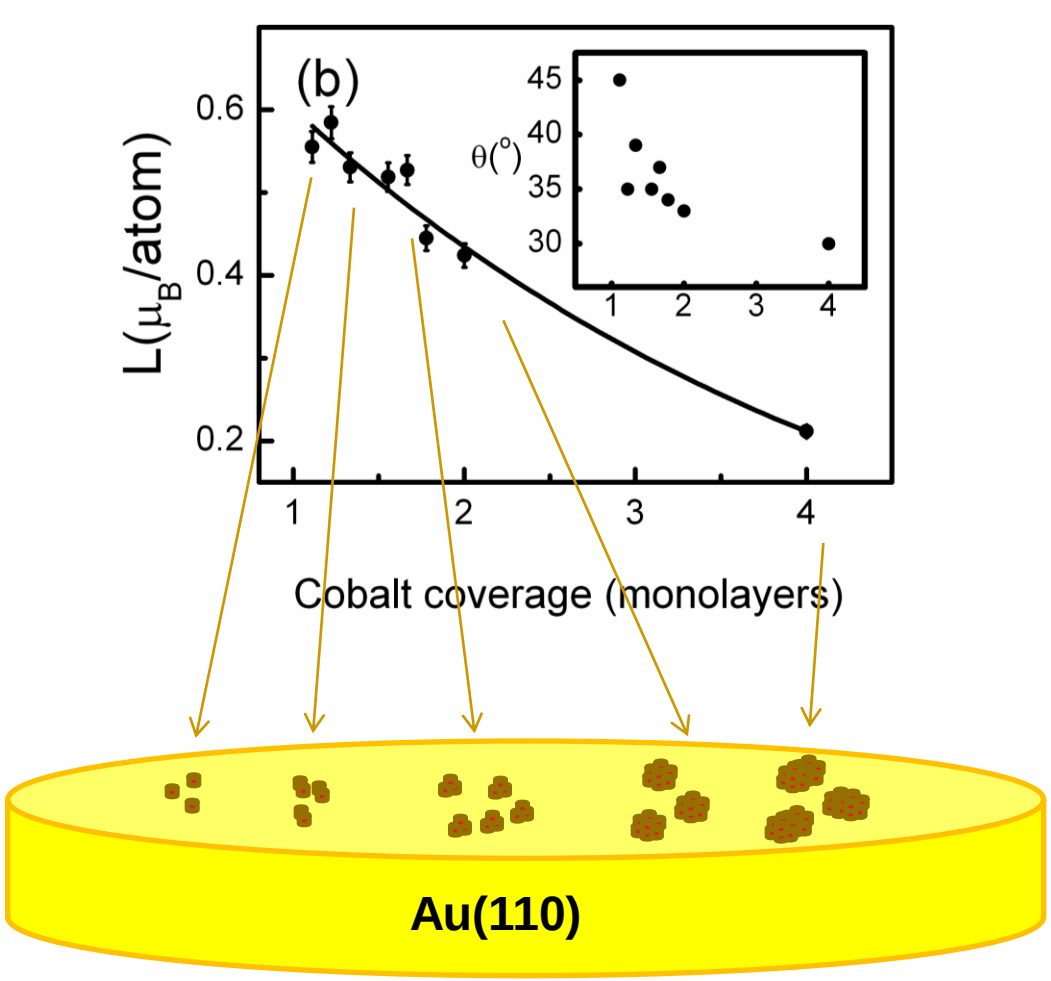

High coordination
Number m_L → 0

Large orbital momentum of Cobalt nanoparticles

m_L (bulk Co) → 0.2

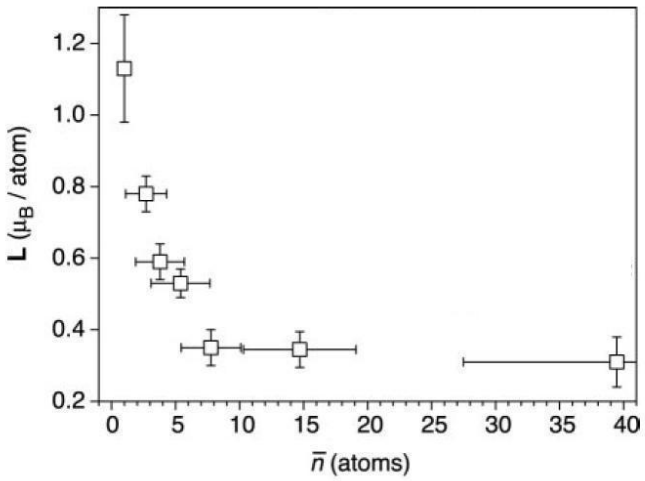

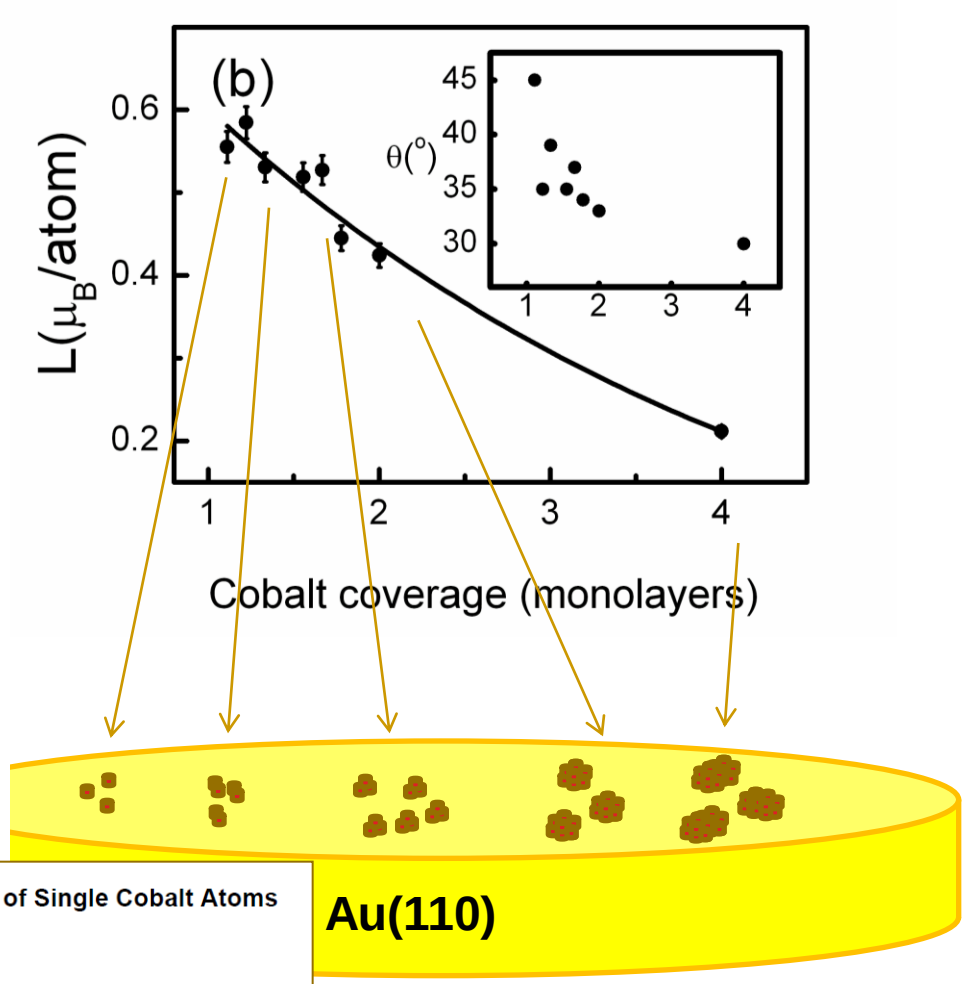

Science
AAAS

Giant Magnetic Anisotropy of Single Cobalt Atoms and Nanoparticles
P. Gambardella, *et al.*
Science **300**, 1130 (2003);
DOI: 10.1126/science.1082857

UFMG

High coordination
Number m_L → 0

LNLS

2C. Magnetic domain reconfiguration in MnAs/GaAs(001) films

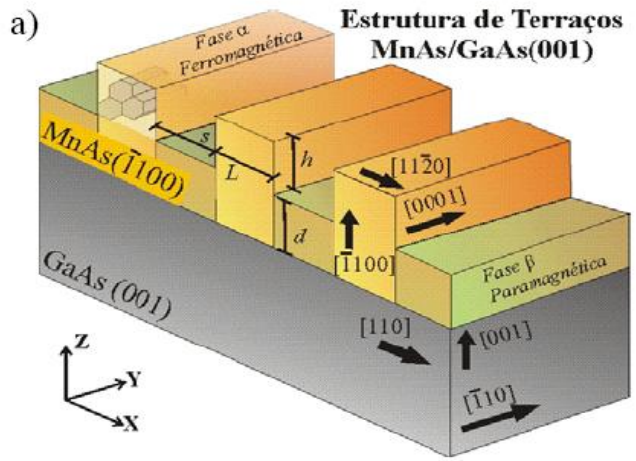

Atomic Force Microscopy (Topography)

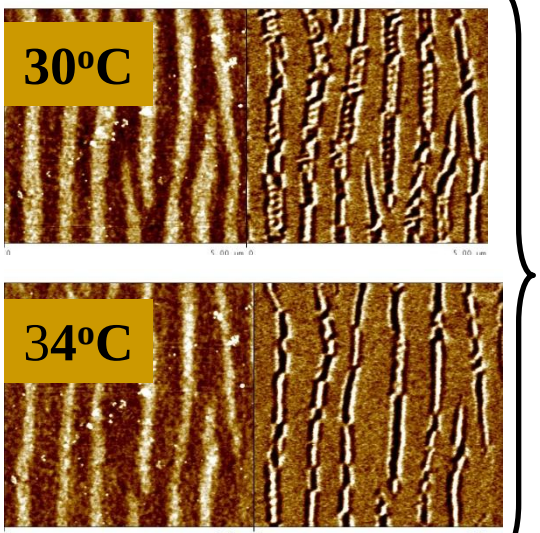

Magnetic Force Microscopy (Magnetic Boundaries)

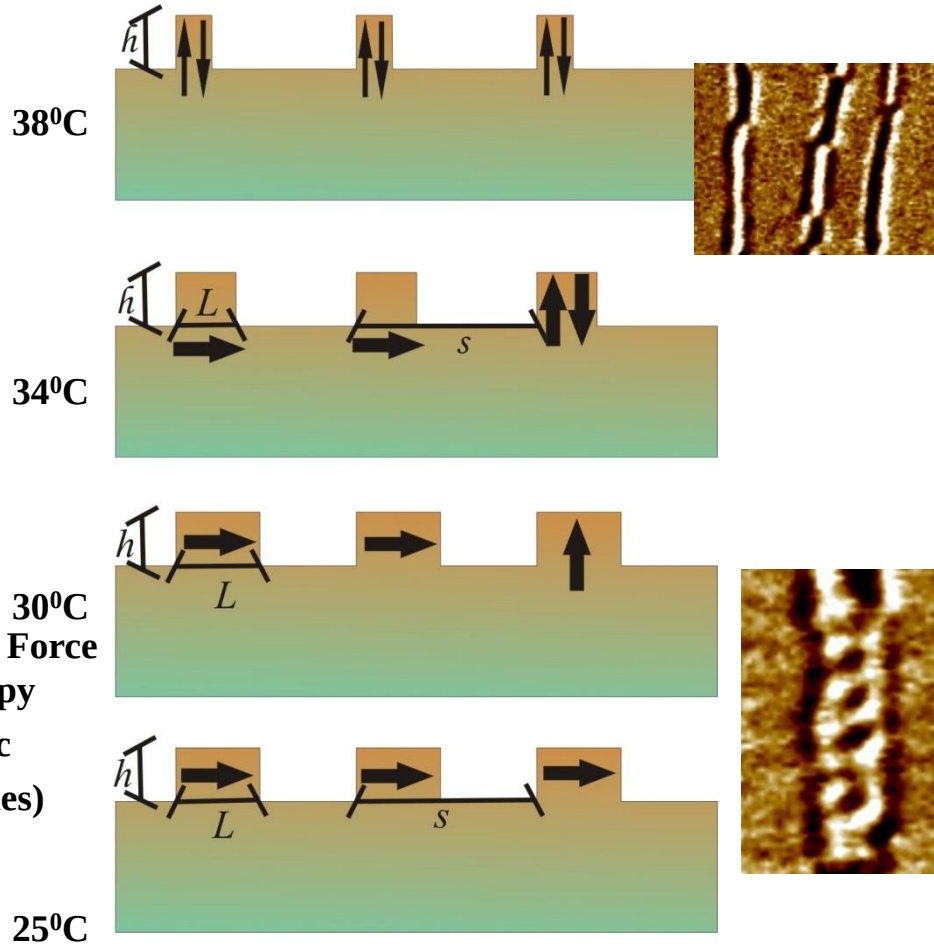

MFM - The magnetic profile changes at about T = 31ºC:

Meanders → Line-shaped structures

2C. Magnetic domain reconfiguration in MnAs/GaAs(001) films: Terrace structure

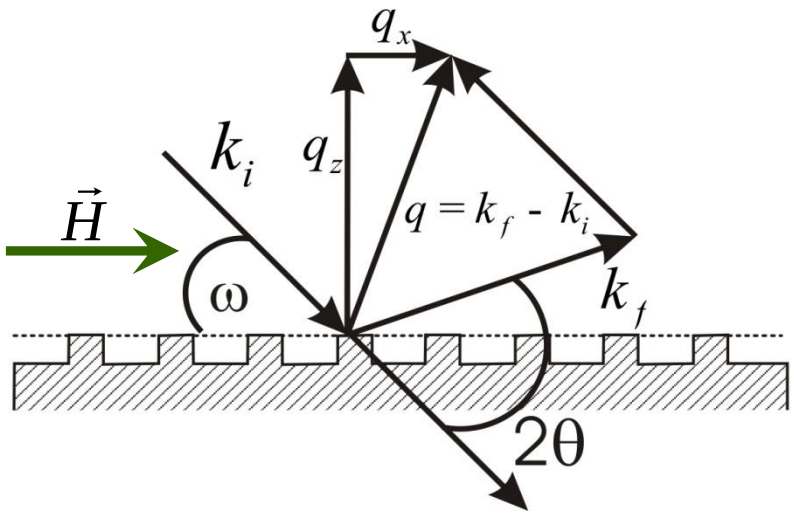

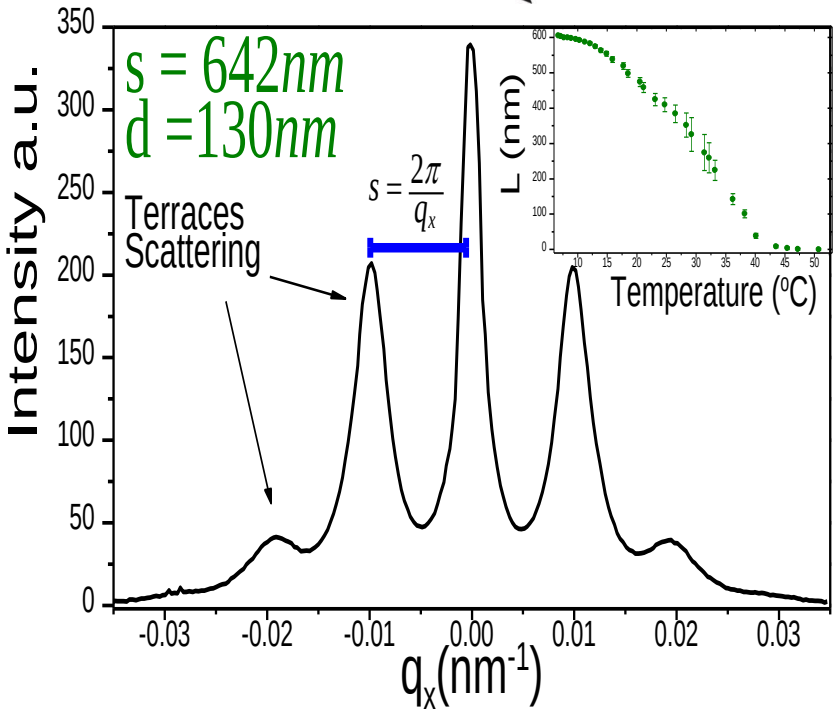

- q_x : terraces period;
- q_z : terraces height;
- Elastic scattering:
- Rocking scans.

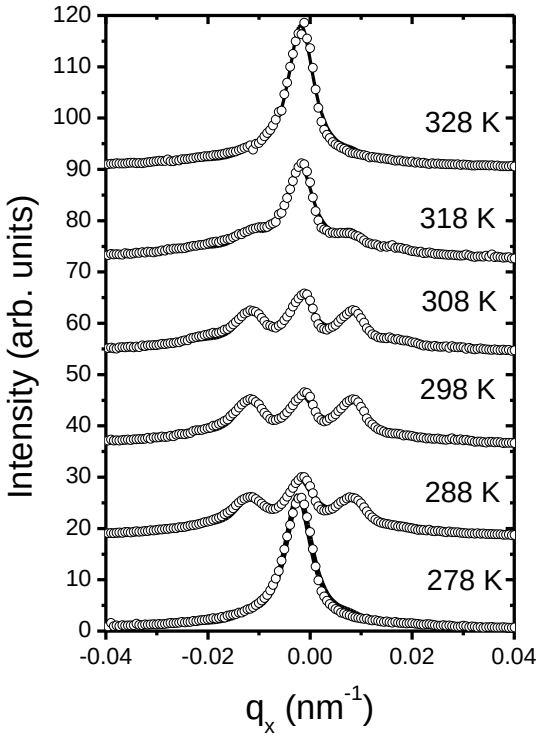

Appl. Phys. Lett. (2005)

2C. Magnetic domain reconfiguration in MnAs/GaAs(001) films
X-Ray Magnetic Resonant Scattering: Polarization and Energy

Near the ressonance, charge scattering increases considerably. Magnetic effects are noticeable, as large as 7% at the Mn L_{III} edge (639eV).

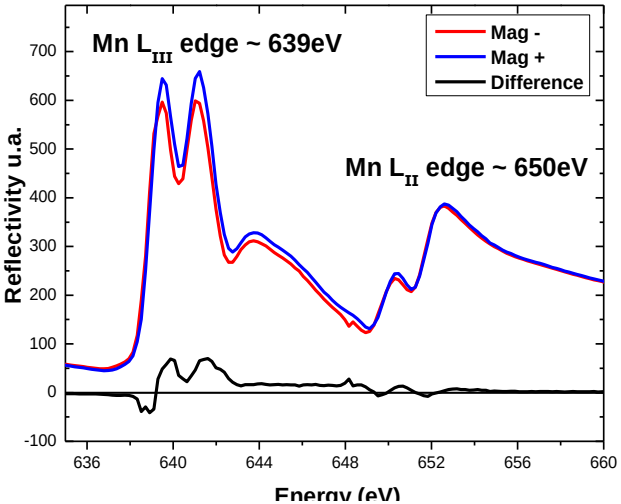

Depending on the polarization, different magnetization directions are probed.

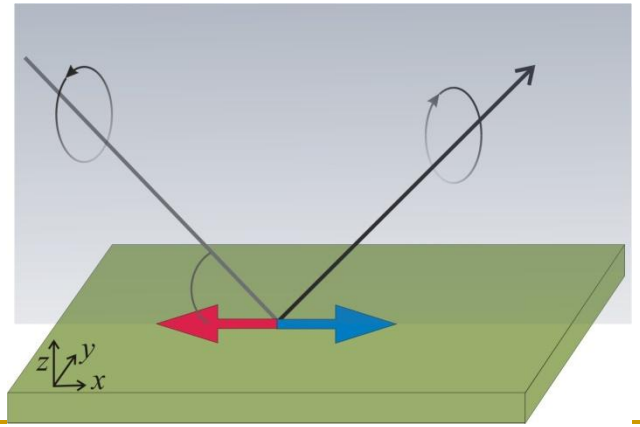

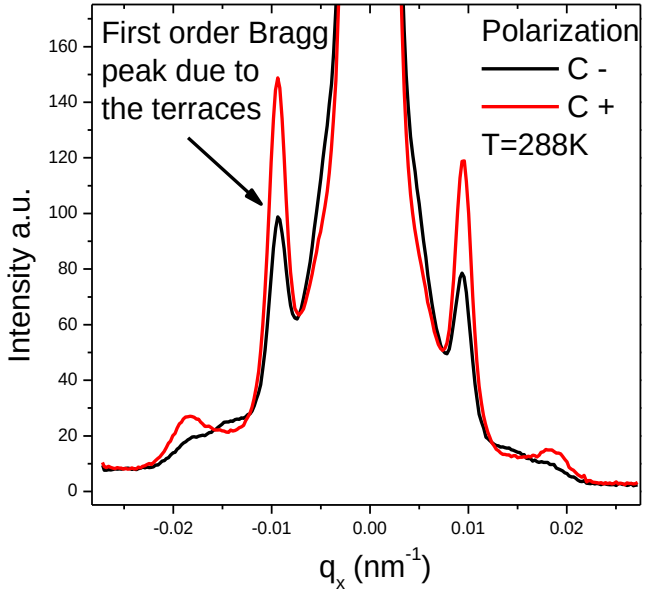

UFMG

LNLS

2C. MnAs/GaAs(001) films: terrace structure and Magnetic Hysteresis measured by resonant magnetic X-ray scattering

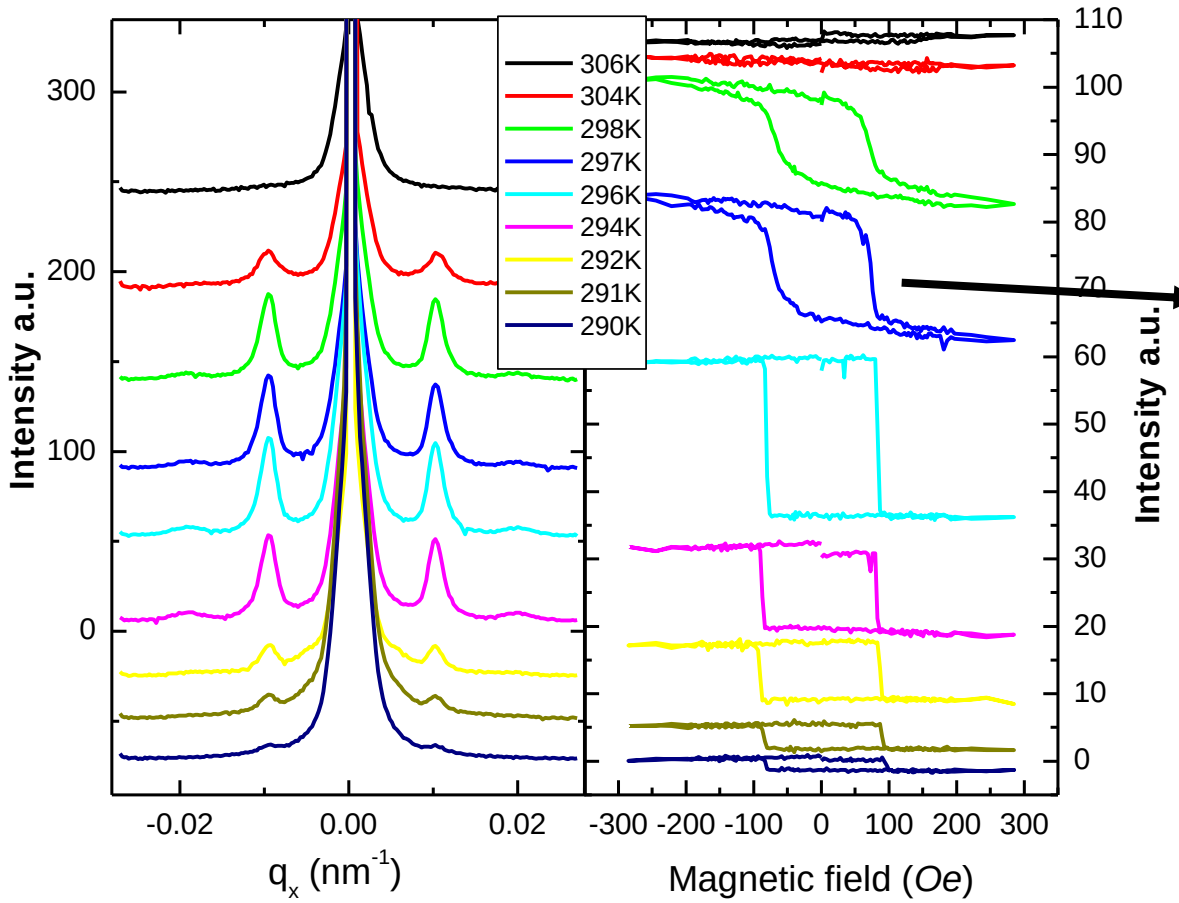

Change in hysteresis lineshape !!!

Hysteresis and rocking curves were done as function of temperature.

2C. MnAs/GaAs(001) films: Magnetic Hysteresis measured by resonant magnetic X-ray scattering

Shrinking of ferromagnetic terrace → Reconfiguration of magnetic domains

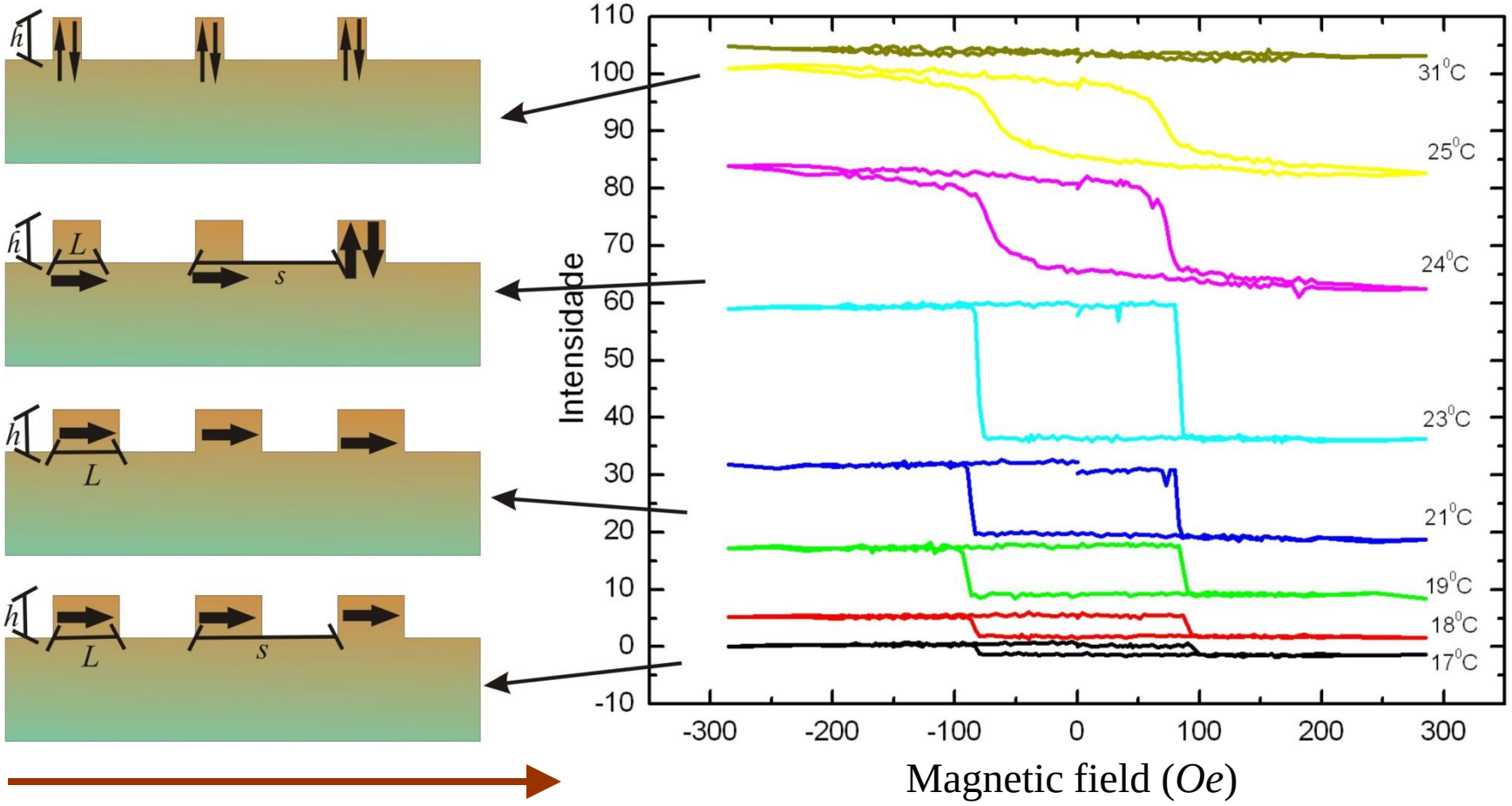

UFMG

LNLS

2C. Magnetic force micorsopy of MnAs/GaAs(001) film

Shrinking of magnetic terrace → Reconfiguration of magnetic domains!

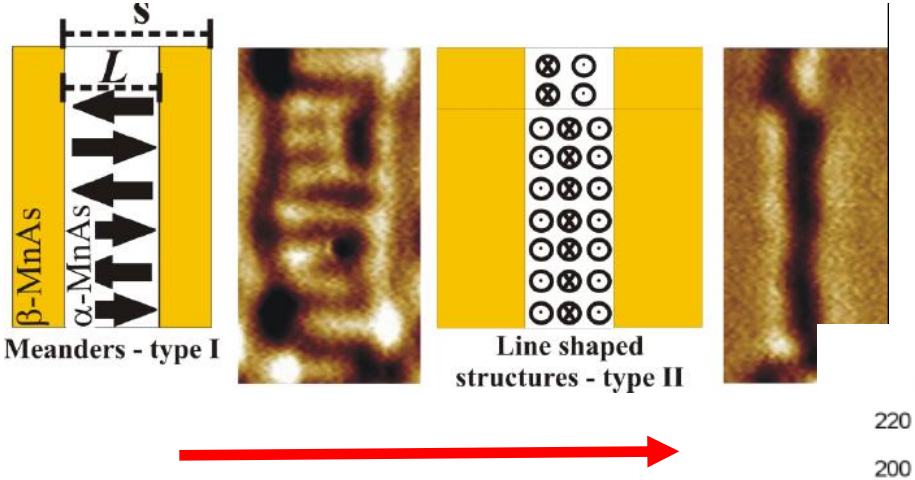

Thermodynamic model of magnetic reconfiguration (p = 2.6)
(J. Appl. Phys. 2006)

Calculation of demagnetization energy

$$E_M = -\frac{1}{2}\int \mathbf{M}\cdot\mathbf{H}_{in}\,'d^3r$$

$$\mathbf{H}'_{in} = -\gamma_B D\cdot\mathbf{M}.$$

$$D_{zz}^{(N)}(p) = \frac{4}{\pi}p\int_0^\infty \tan^2\left(\frac{\xi}{2p}\right)\left[1-(-1)^N\cos(\xi)\right]\sinh\left(\frac{\xi}{2p}\right)d\xi$$

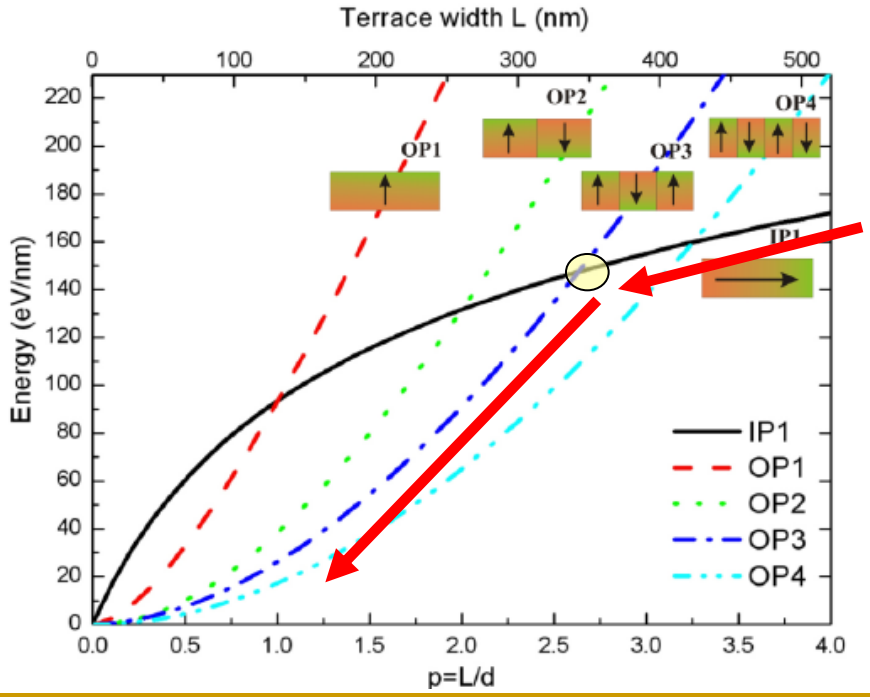

UFMG

LNLS

2C. MnAs/GaAs(001) films: Magnetic Hysteresis measured by resonant magnetic X-ray scattering

$$E(p,\varphi,H)=\left[\frac{1}{2}M^2 4\pi\left(D_{zz}^{(3)}(p)-D_{xx}^{(1)}(p)\right)\right]\sin^2\varphi - HM\cos\varphi\,,$$

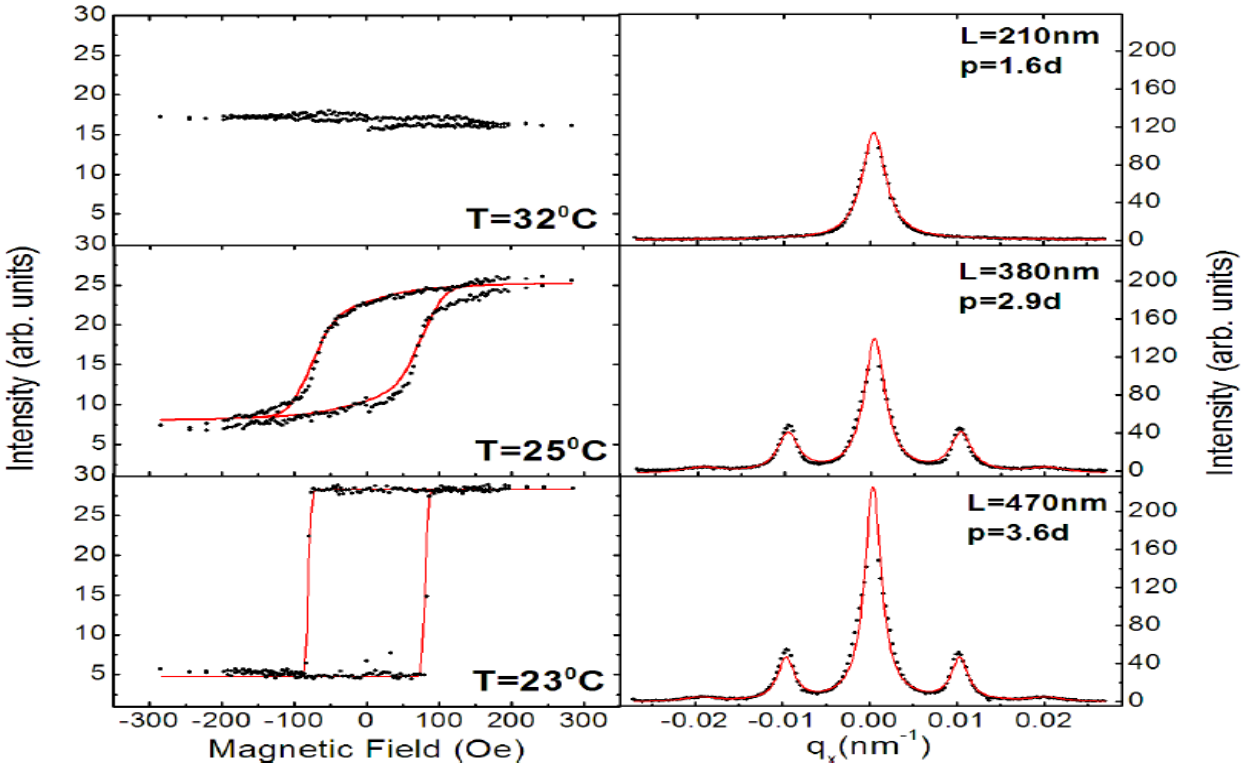

Thermodynamic model of magnetic reconfiguration (J. Appl. Physics 2006)

2D. Fe/MnAs films: chemical sensitivity using resonant magnetic X-ray scattering

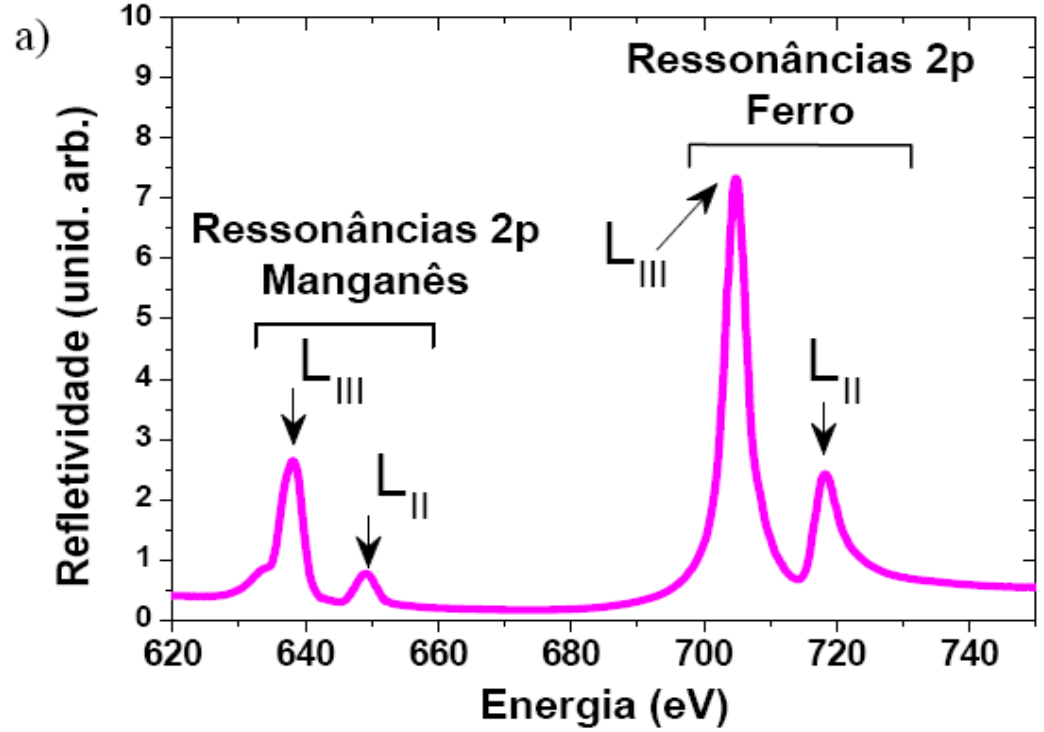

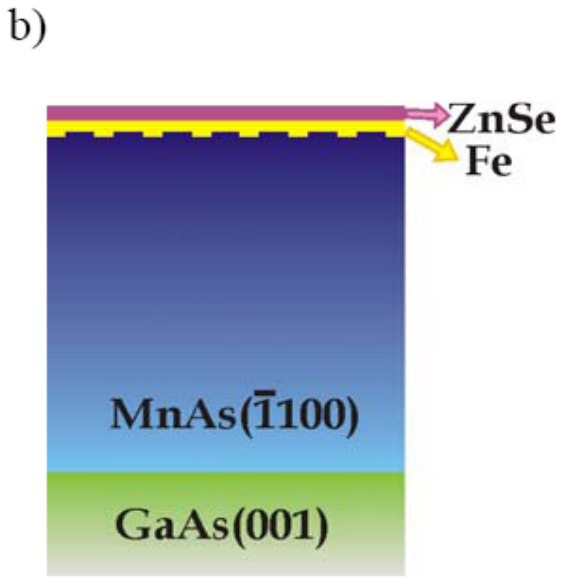

Mn L_3 edge → 640eV, Fe L_3 edge → 707eV

D. Fe/MnAs films: magnetic hysteresis measured by magnetic resonant X-ray scattering. Each scans is performed at two different absorption edges: Fe and Mn !!!

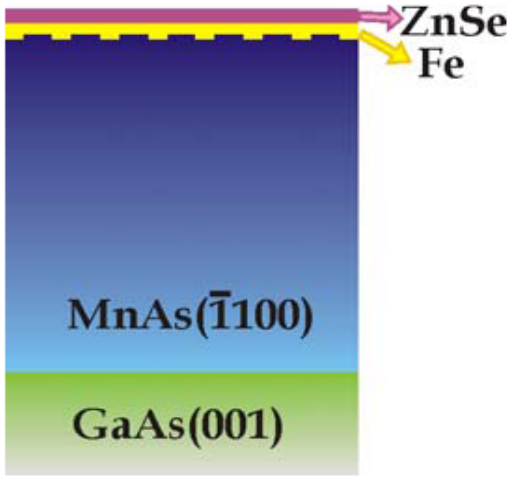

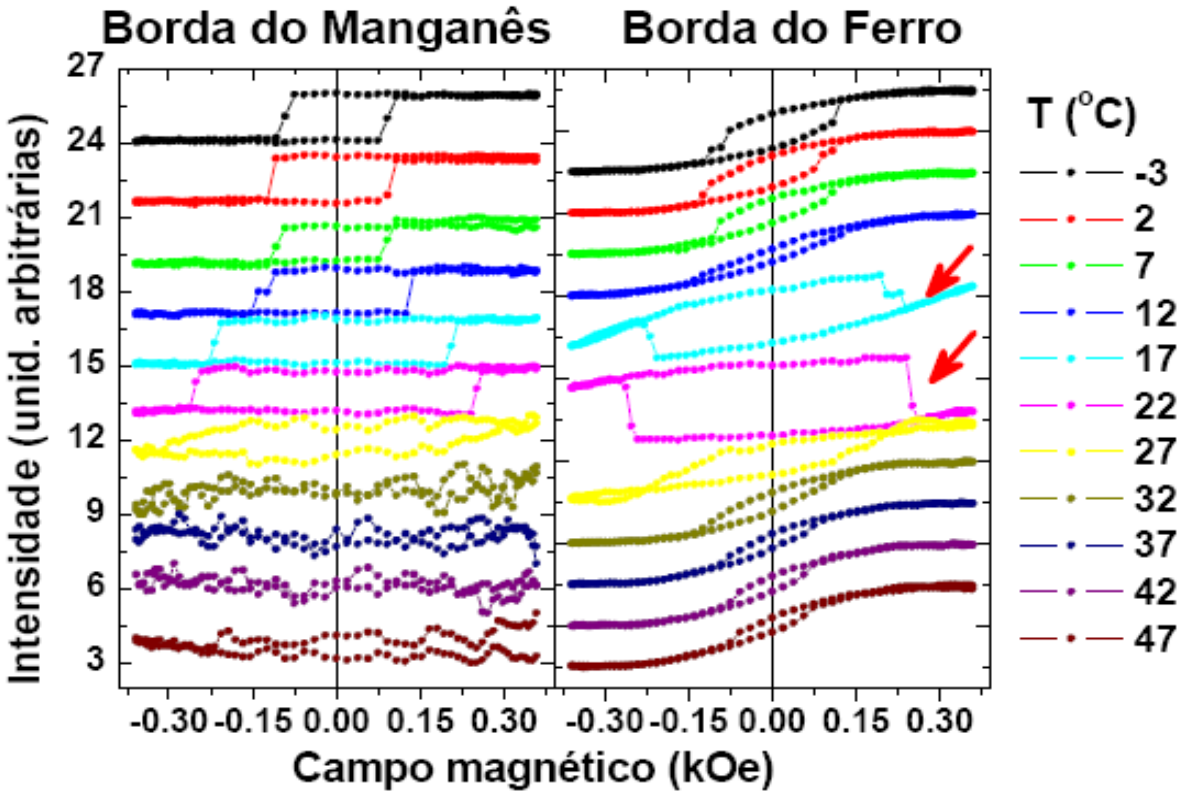

Mn – 640eV

Fe – 707eV

UFMG

LNLS

2D. Fe/MnAs films: Magnetic Hysteresis measured by resonant magnetic X-ray scattering: magnetic coupling between MnAs teraces and Fe film.

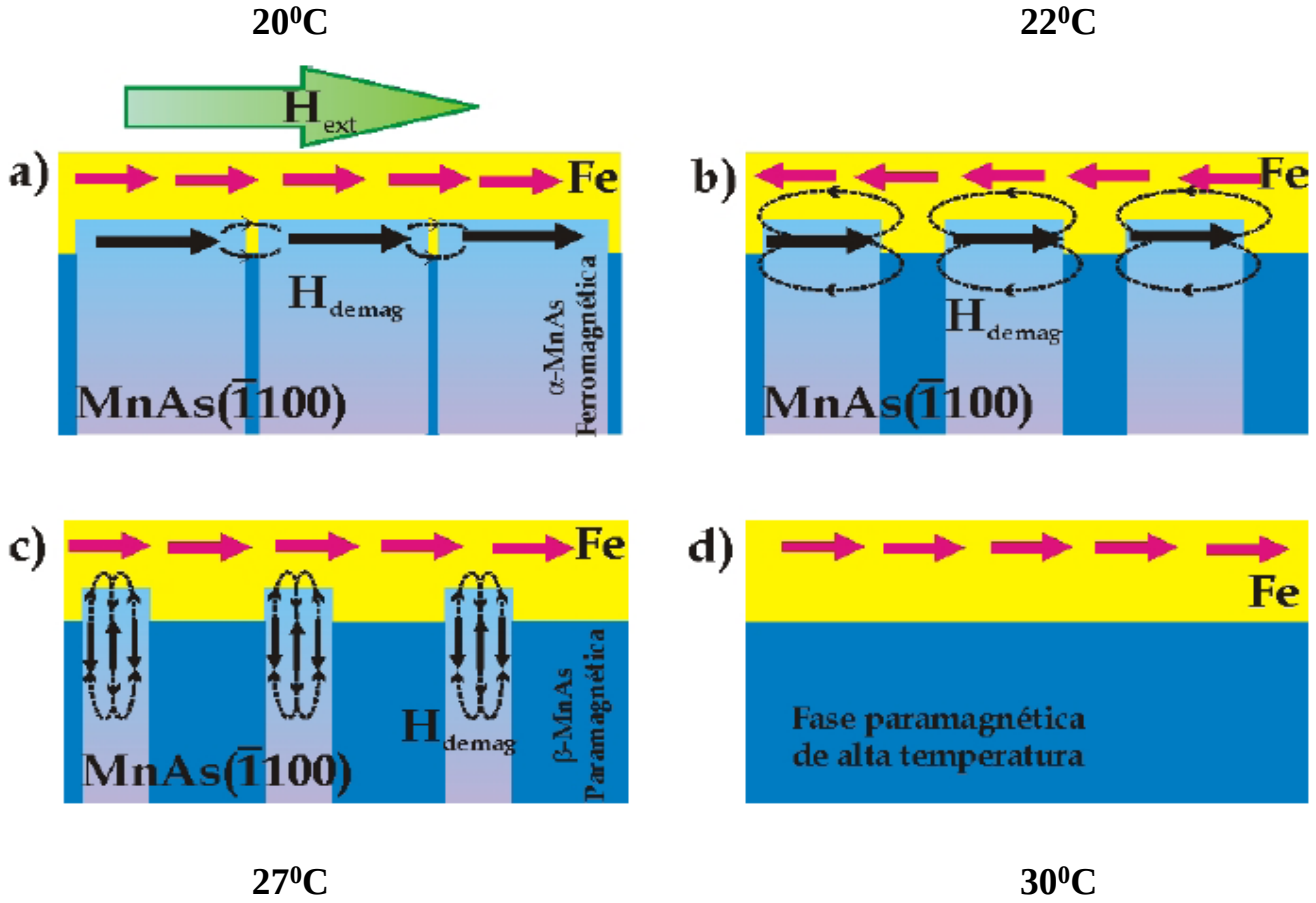

Can we make a thermodynamic model of magnetic reconfiguration (current research) ?

2E. Microscopy with magnetic domain sensitivity

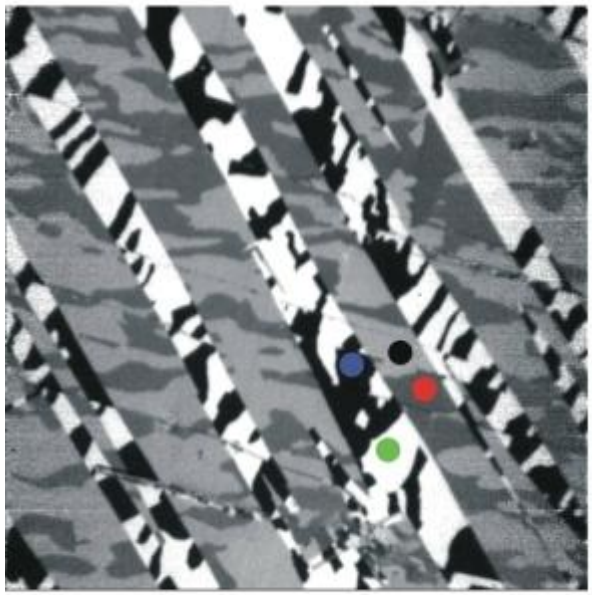

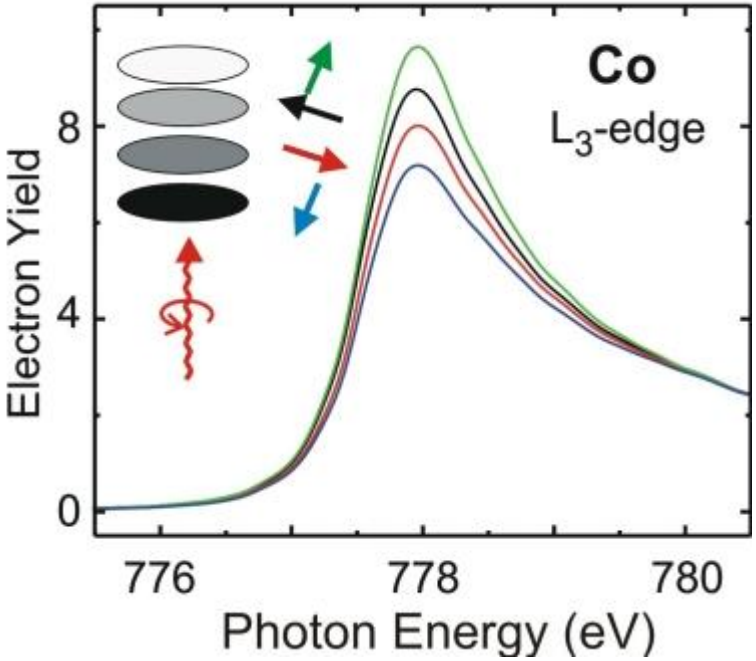

Ferromagnetic domain pattern for a thin Co layer on NiO(100), showing all four spin directions in Co. The spin directions are pinned by the underlying NiO.

UFMG

LNLS

4. Conclusions

- **X-ray magnetic circular dichroism reveals magnetism with chemical specificity**
- **Orbital and spin moments can be determined separately**

- Anomalous Palladium magnetism in nanostructures

- Giant orbital magnetic moment of Co/Au nanostructures

- Magnetic domain reconfiguration in MnAs/GaAs films

- Fe/MnAs magnetic coupling

- Microscopy with magnetic domain sensitivity

Acknowledgements

- **Daniel Bretas, Letícia Coelho (DF-UFMG)**
- **Harry Westfahl (LNLS, Campinas)**
- **Maurizio Sacchi (SOLEIL, France)**

Thanks: ABTLuS, CNPq, FAPESP, FAPEMIG

UFMG

LNLS